Antimatter in cosmic rays: The role of cross section

Fiorenza Donato

Torino University & INFN

Cern 22.06.2022 - Fixed target at the LHC

CRs in the Galaxy

Primaries: produced in the sources (SNR and Pulsars)

H, He, CNO, Fe; e−, e+; possibly e^+, p^-, d^- from Dark Matter annihilation

Secondaries: produced by spallation of primary CRs (p, He,C, O, Fe) on the interstellar medium (ISM): Li, Be, B, sub-Fe, [...], (radioactive) isotopes ; e^+, p^-, d^-

At first order, we understand fluxes at Earth as shaped by few, simple, isotropic effects:

- acceleration in shocked stellar environments (SNR, PWN)
- particle interactions between CRs and ISM (scross sections)
- diffusion of the galactic magnetic fields
- particle energy losses
- Fusion (antinuclei)

Precision data from space: nuclei, electrons

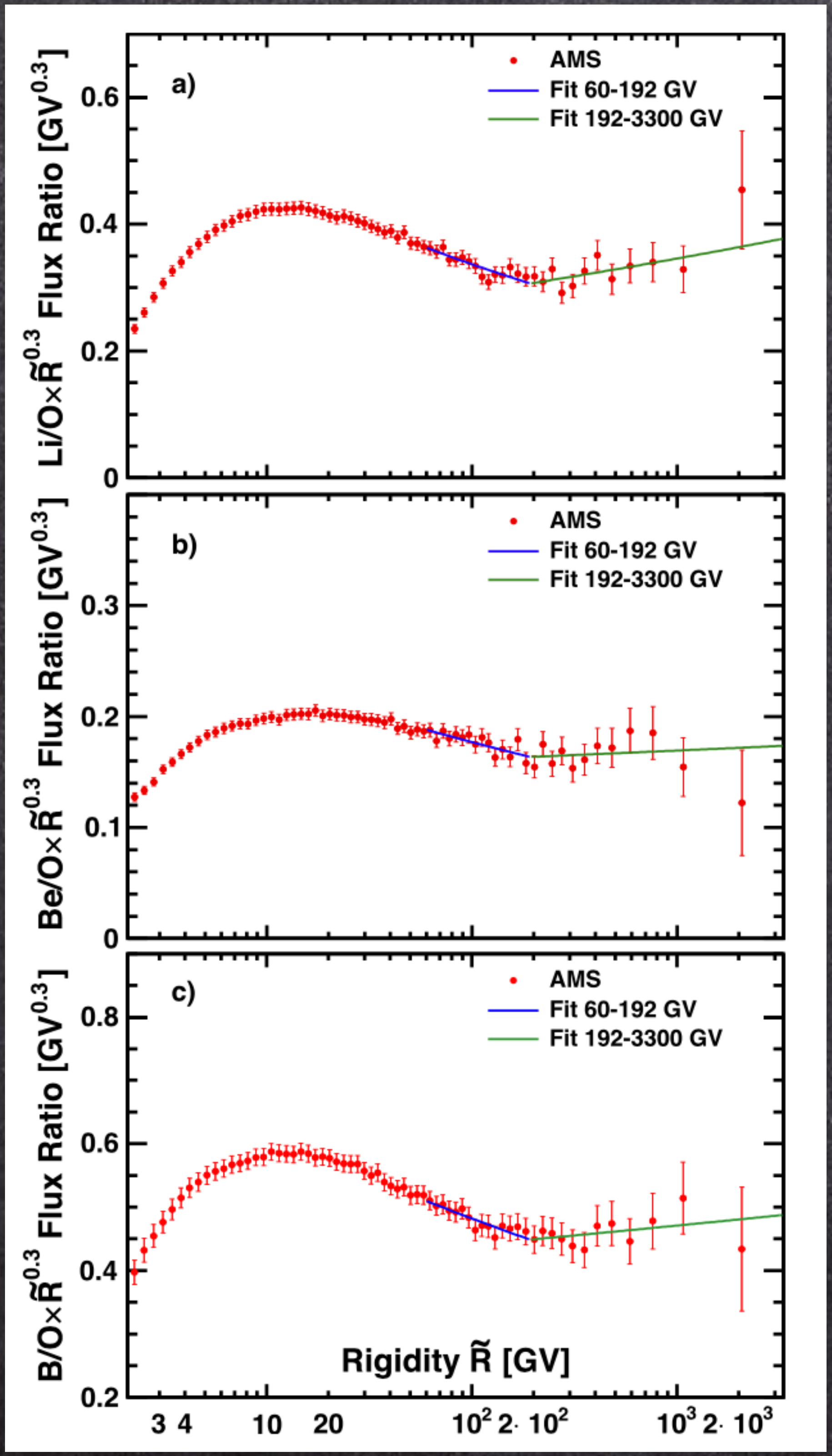

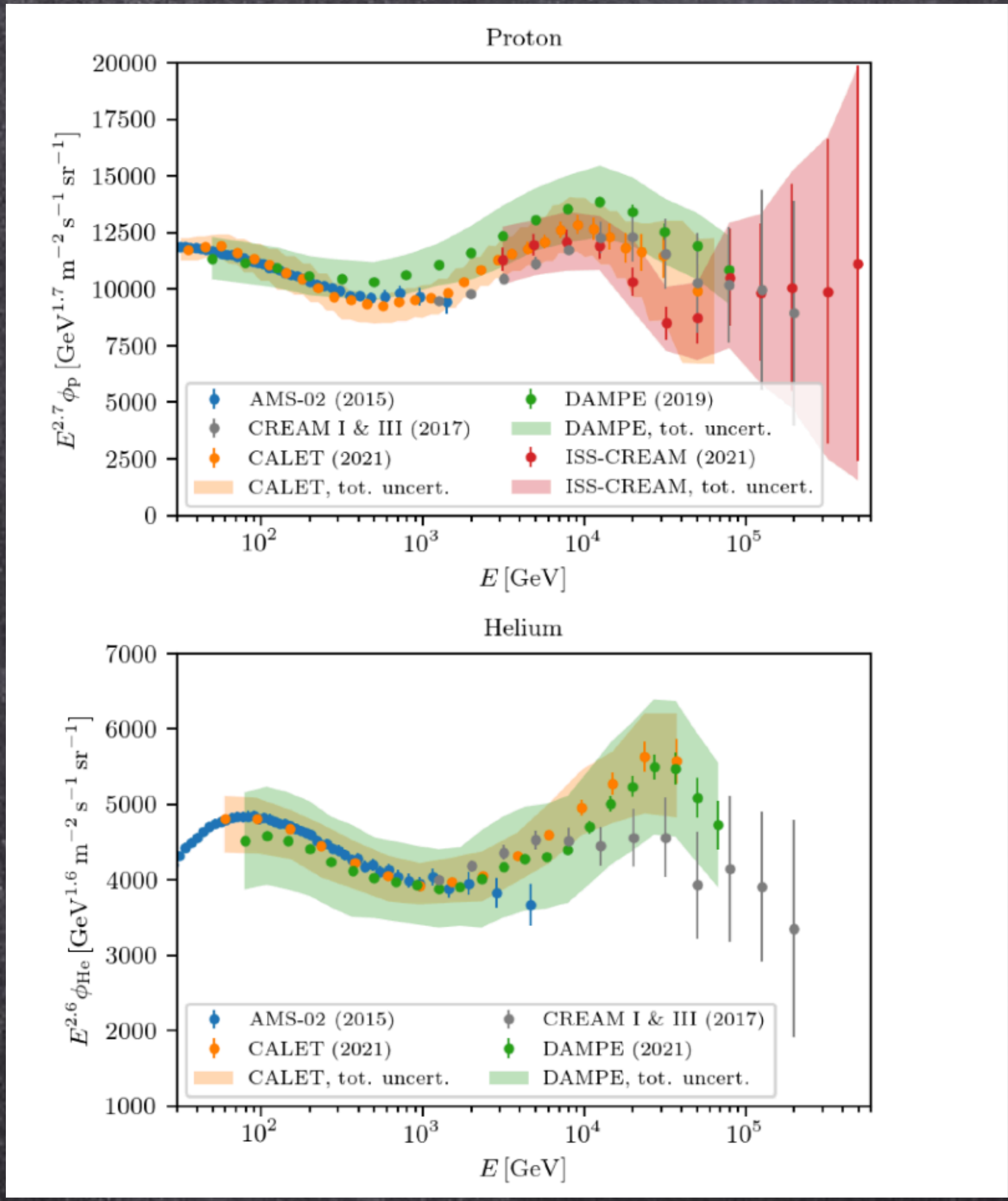

Propagation equation

$$\frac{\partial \psi}{\partial t} - \nabla \cdot \{D(E) \nabla \psi\} + \frac{\partial}{\partial E}\left\{\frac{dE}{dt}\psi\right\} = Q(E, \mathbf{x}, t)$$

diffusion en. losses source spectrum

Diffusion: D(x,R) a priori
usually assumed isotropic in the Galaxy: $D(R)=D_0R^{\delta}$
D_0 and δ usually fixed by B/C (kappl+15; Genolini+15 (K15))

Energy losses: Synchrotron on the galactic B~3.6 μG
full relativistic of Compton effect (w/ Klein-Nishijna)
on photon fields (stellar, CMB, UV, IR)

Solution of the eq.: semi-analytic (Maurin+ 2001, Donato+ 2004, ...), USINE codes
or fully numerical: GALPROP, DRAGON codes

Geometry of the Galaxy: cylinder with height L

Antimatter or γ-rays sources from DARK MATTER

Annihilation

$$Q_{\rm ann}(\vec{x},E) = \epsilon \left(\frac{\rho(\vec{x})}{m_{DM}}\right)^2 \sum_f \langle \sigma v\rangle_f \frac{dN^f_{e^\pm}}{dE}$$

Decay

$$Q_{\rm dec}(\vec{x},E) = \left(\frac{\rho(\vec{x})}{m_{DM}}\right) \sum_f \Gamma_f \frac{dN^f_{e^\pm}}{dE}$$

- ρ DM density in the halo of the MW
- m_{DM} DM mass
- $\langle \sigma v \rangle$ thermally averaged annihilation cross section in SM channel f
- Γ DM decay time
- e+, e- energy spectrum generated in a single annihilation or decay event

Propagation models vs data

Korsmeier & Cuoco, PRD 2021

Several propagation models are tested

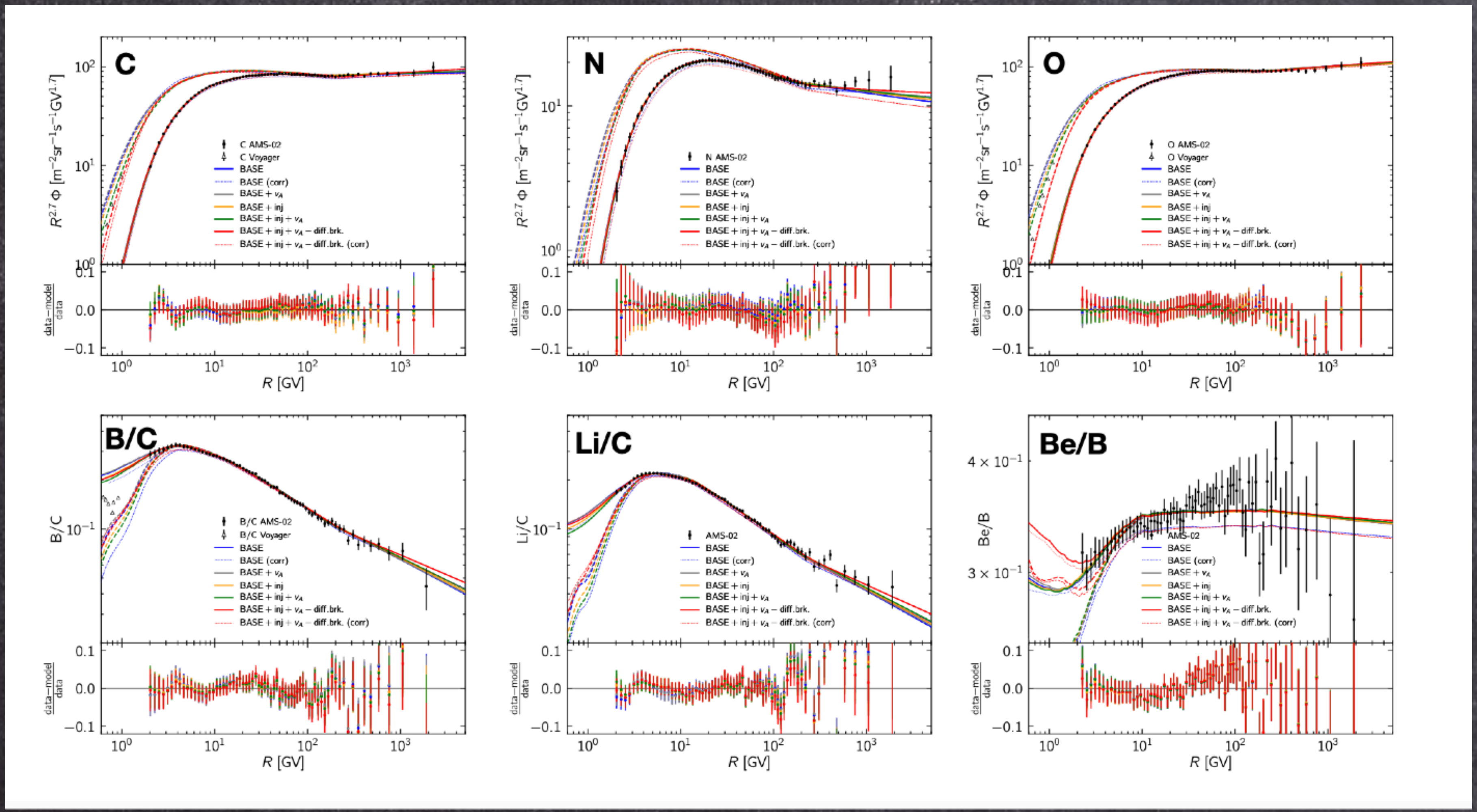

Fragmentation cross section uncertainties currently prevent a better understanding of CR propagation

Fragmentation cross sections

They matter in both directions: as a loss term for progenitors, as a source term for daughters

De La Torre Luque+ JCAP 2021

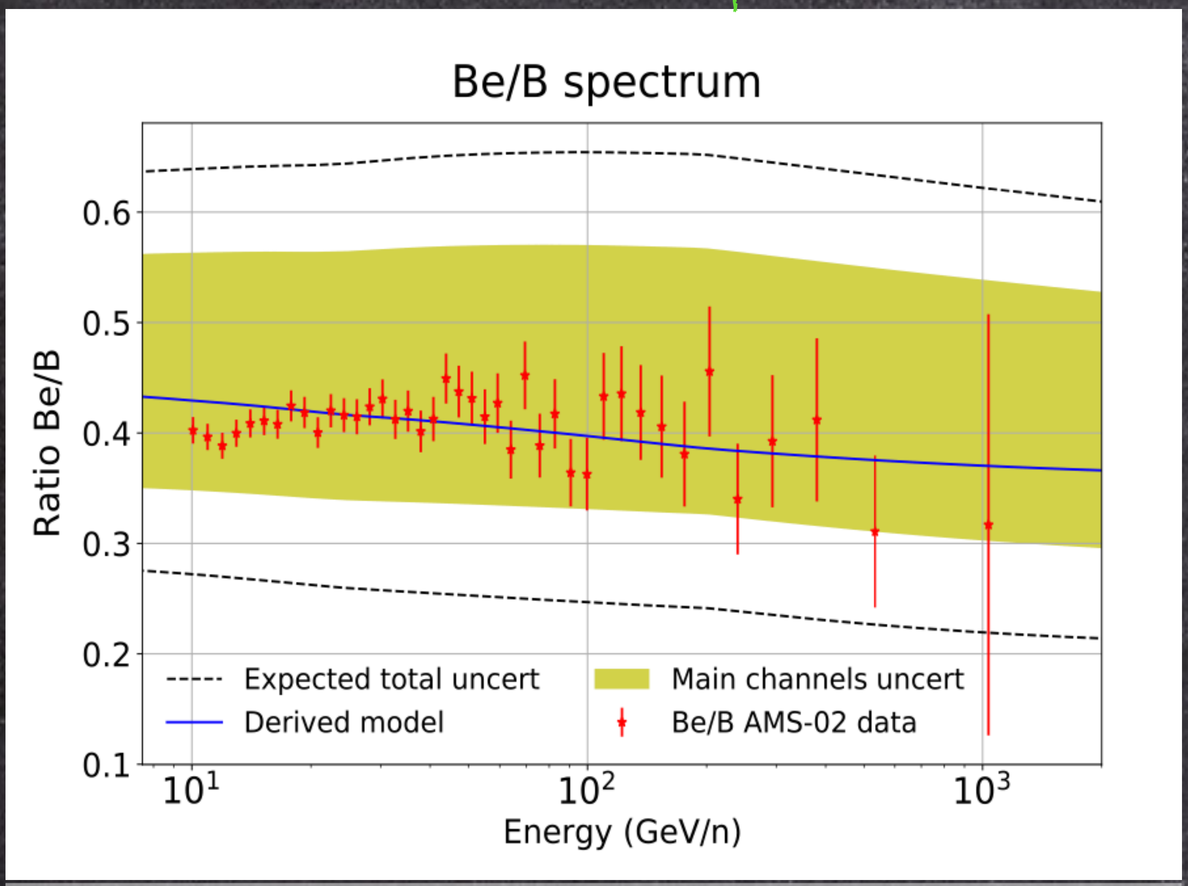

Weinrich+ A&A 2021

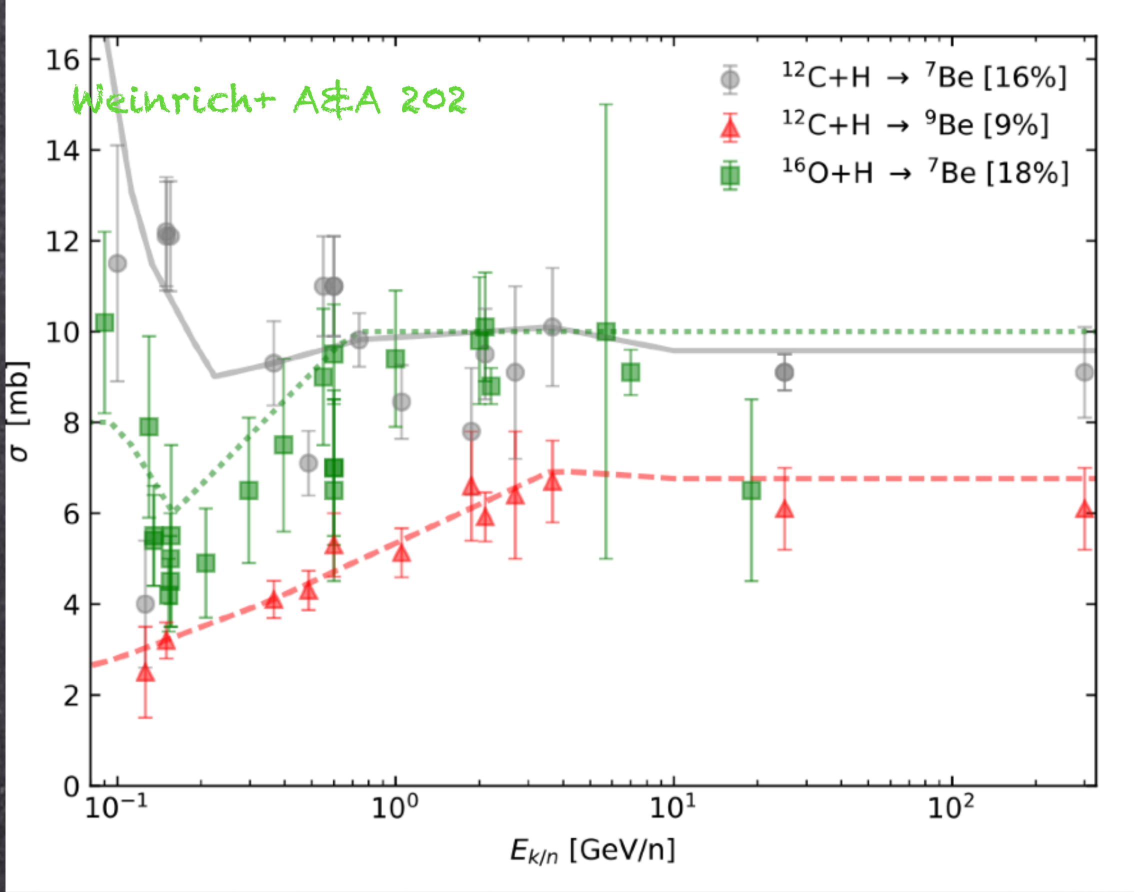

Probably the most limiting aspect now

Dedicated campaigns are needed (LHCb, NA61, Amber/Compass, ...)

The case for antiprotons

AMS-02 antiprotons are consistent with a secondary astrophysical origin

M. Boudaud, Y. Genolini, L. Derome, J.Lavalle, D.Maurin, P. Salati, P.D. Serpico PRD 2020

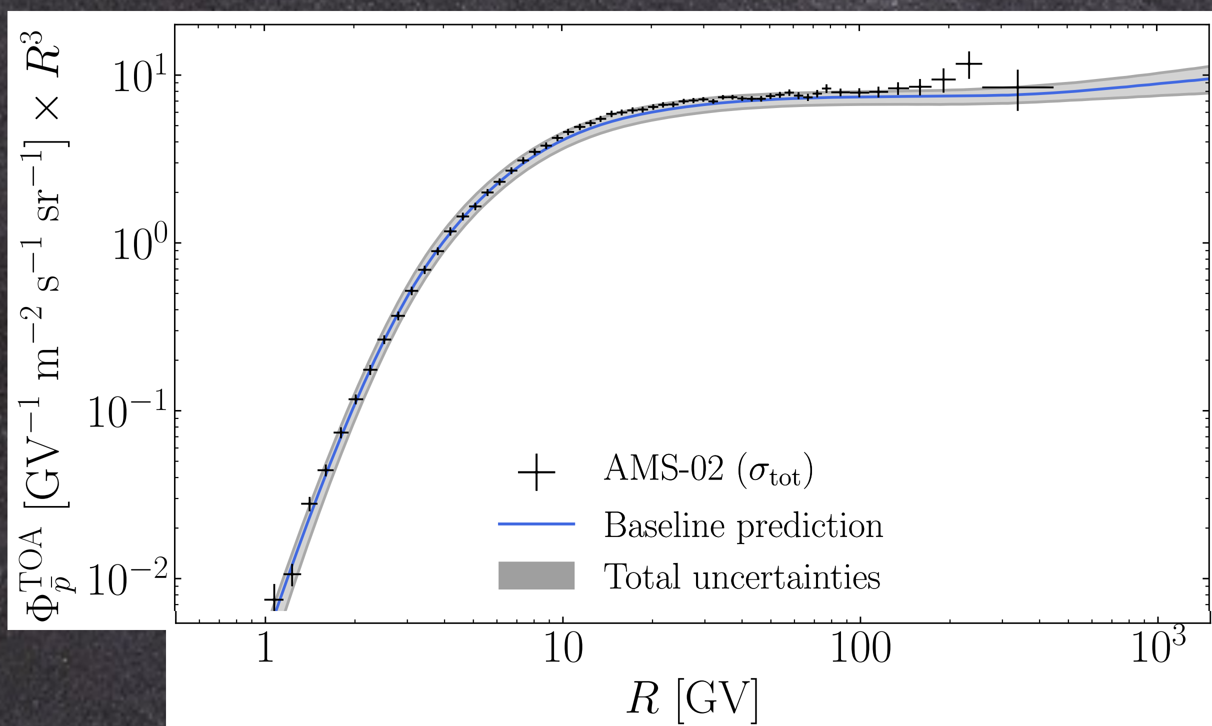

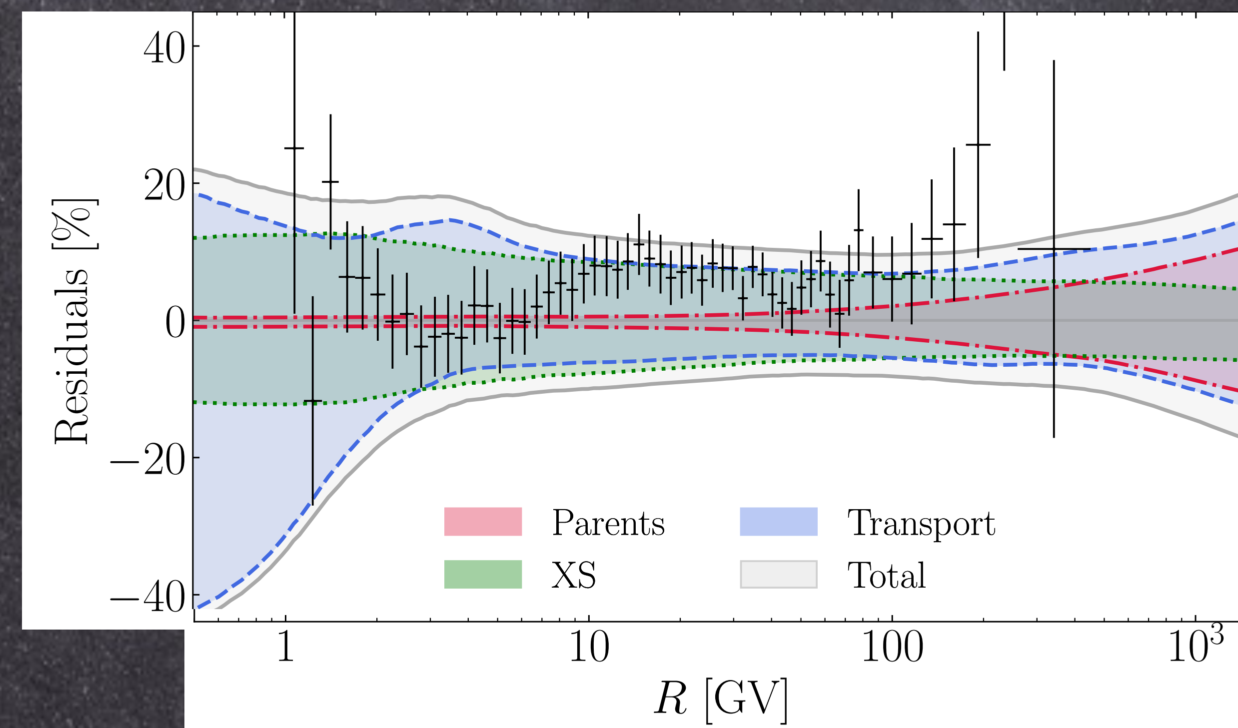

Secondary pbar flux is predicted consistent with AMS-02 data

A dark matter contribution would come as a tiny effect

Transport and cross section uncertainties are comparable

New fixed-target data for the antiproton cross sections

FD, Korsmeier, Di Mauro PRD 2018

pp —> pbar+X	pHe —> pbar + X
NA61 (Aduszkiewicz Eur. Phys. J. C77 (2017))	**LHCb** (Graziani et al. Moriond 2017)
$\sqrt{s}$=7.7, 8.8, 12.3 and 17.3 GeV	$\sqrt{s}$ = 110 GeV
T_p = 31, 40, 80, 158 GeV	T_p = 6.5 TeV

Fraction of the pp source term covered by the kinematical parameters space

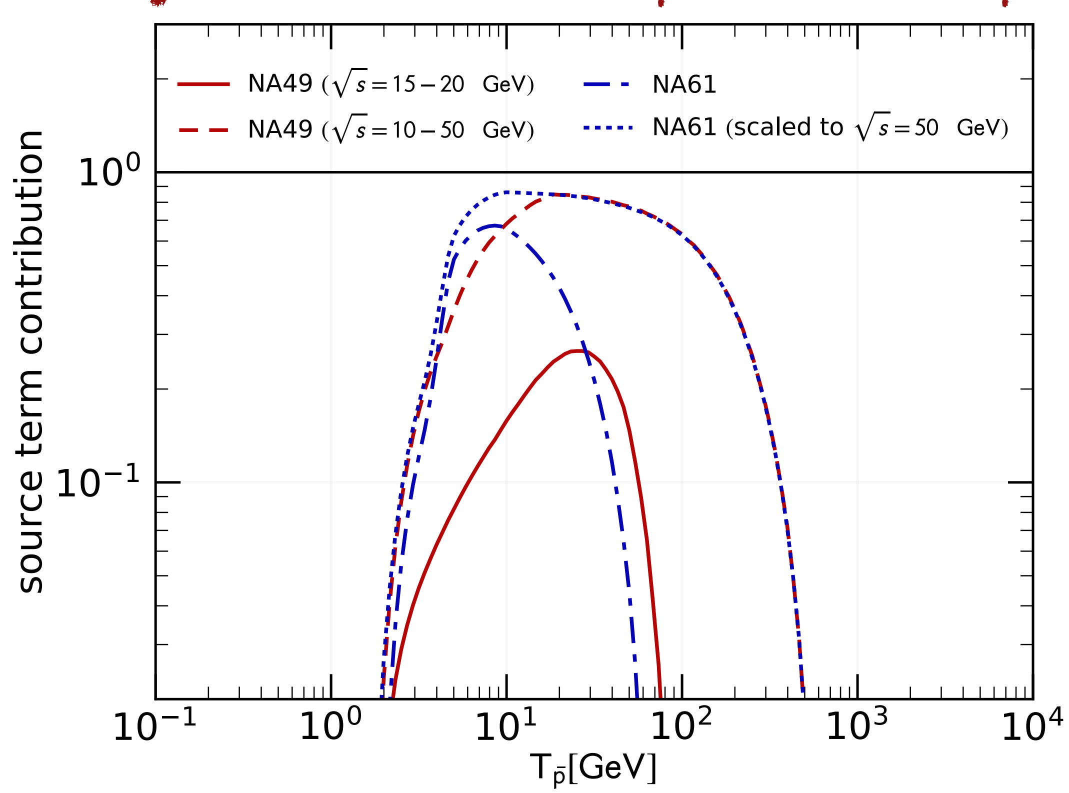

Fraction of the p-nucelus source term covered by the kinematical parameters space

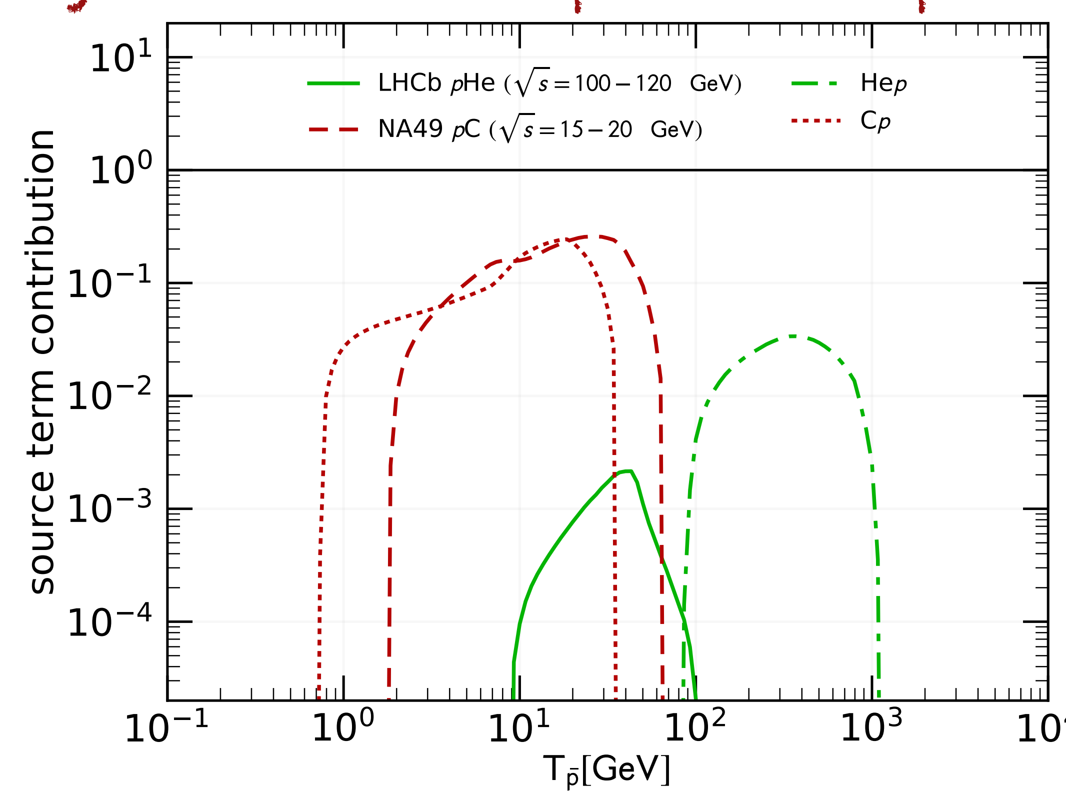

The antiproton source spectrum

Korsmeier, FD, Di Mauro, PRD 2018

pp -> p- X source term

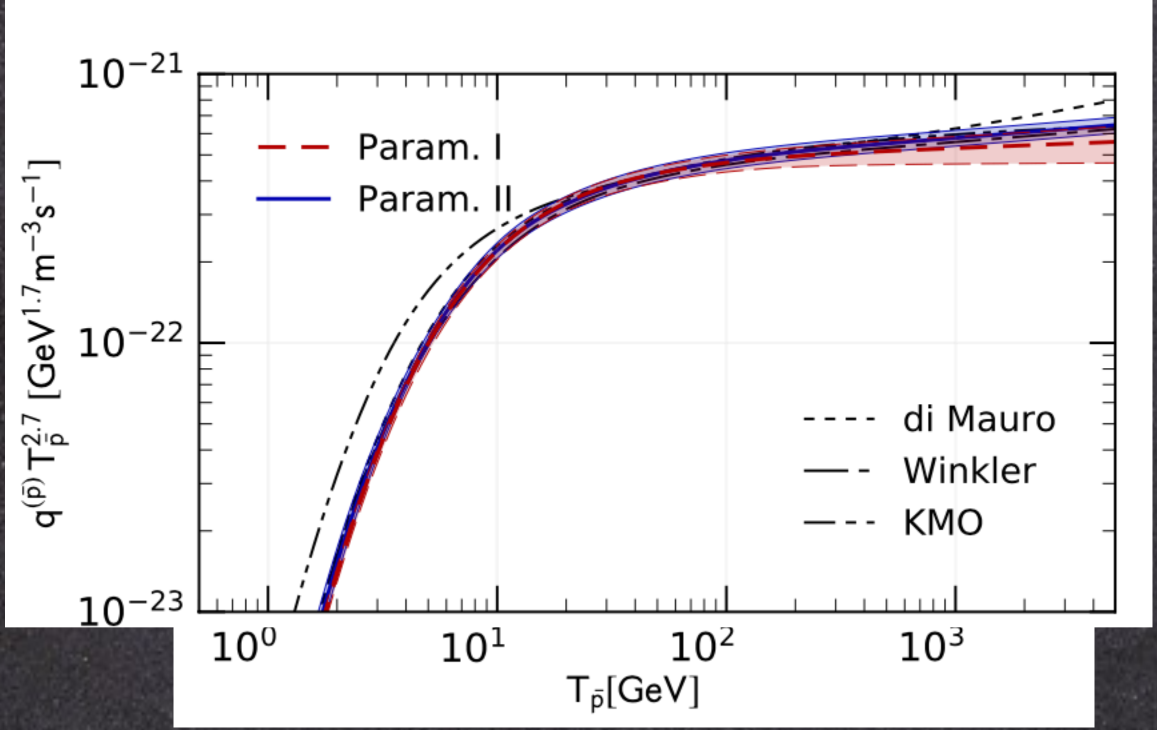

LHCb pHe -> p- X data & our fit

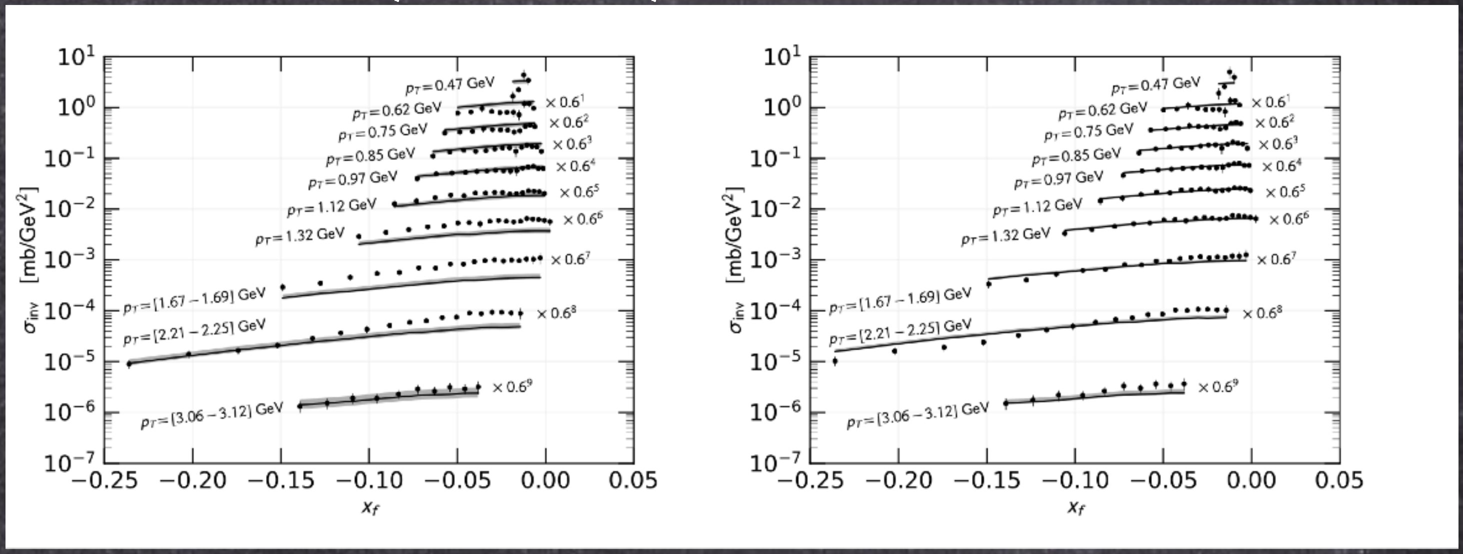

The effect of LHCb data is to select a high energy trend of the pbar source

A harder trend is preferred.

Effects on the total pbar production

Korsmeier, FD, Di Mauro, 1802.03030, PRD 2018

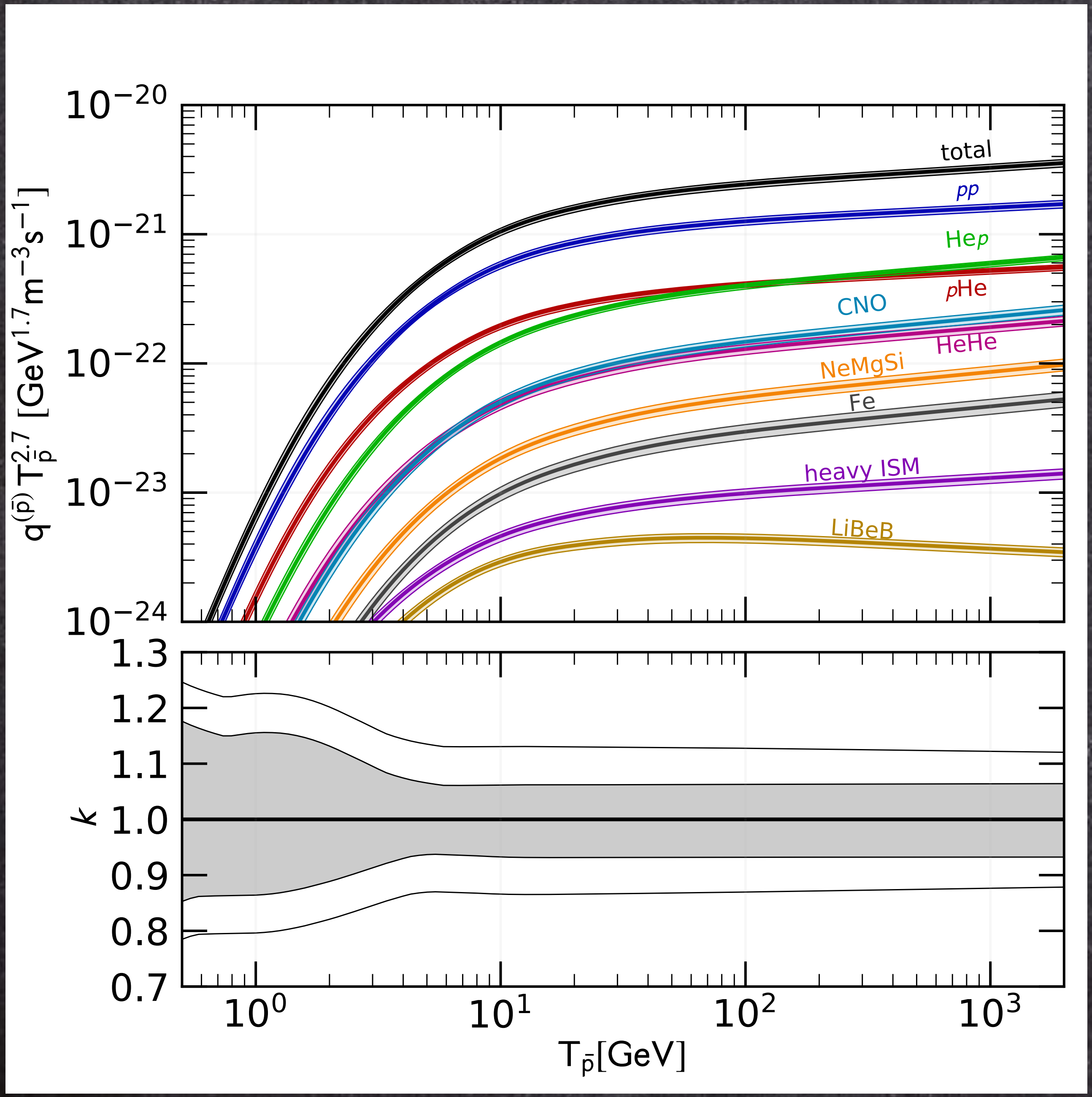

Result with uncertainties in the hyperon correction and isospin violation

The antiproton source term is affected by uncertainties of ± 10% from cross sections.

Higher uncertainties at very low energies

The case for Positrons

The journey started with the attempt to interpret the e+ and e- data

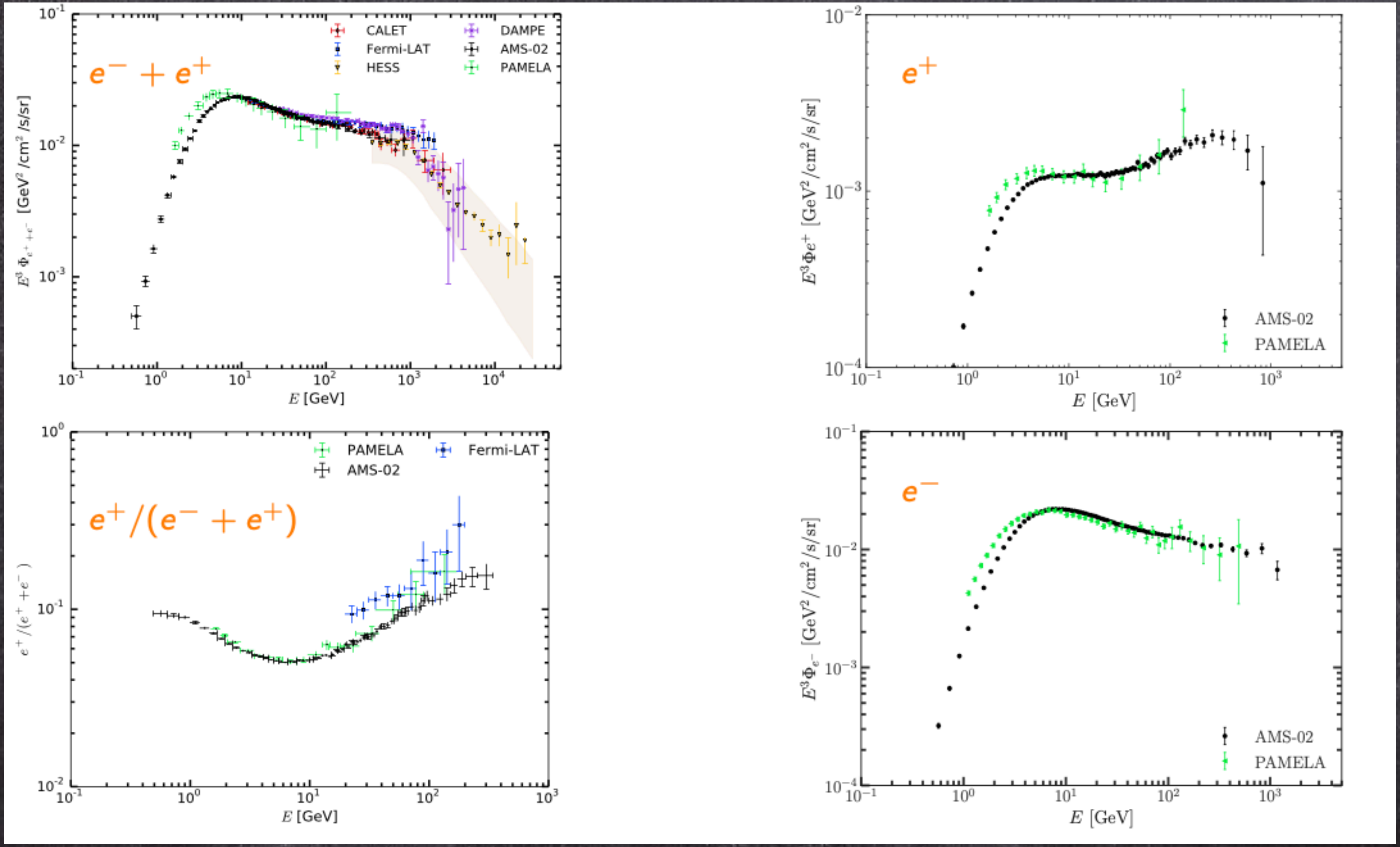

Unprecedented statistics and energy coverage

Main sources of $e^{\pm}$ in the Milky Way
The Q(E, x, t) term

- Inelastic hadronic collisions (asymmetric in e+/e-)
- Pulsar wind nebulae (PWN) (symmetric in e+/e-)
- Supernova remnants (SNR) (only or mostly e-)
- (Particle Dark Matter annihilation)

The secondary, hadronic e± source term

L. Orusa, M. Di Mauro, FD, M. Korsmeier PRD 2022

$$q_{ij}(T_{e^+}) = 4\pi\, n_{\mathrm{ISM},j} \int dT_i\, \phi_i(T_i) \frac{d\sigma_{ij}}{dT_{e^+}}(T_i, T_{e^+})$$

i, j: nuclei. Specifically pp, pHe, Hep, HeHe

n_{ISM}: density of the interstellar medium

$\Phi_i(T_i)$: flux of incoming CR nucleus (~ $T_i^{-2.7}$)

$d\sigma_{ij}/dT_e(T_i,T_e)$; e± production cross section in a ij collision, for a given CR (beam) energy

e+ production channels

L. Orusa, M. Di Mauro, FD, M. Korsmeier PRD 2022

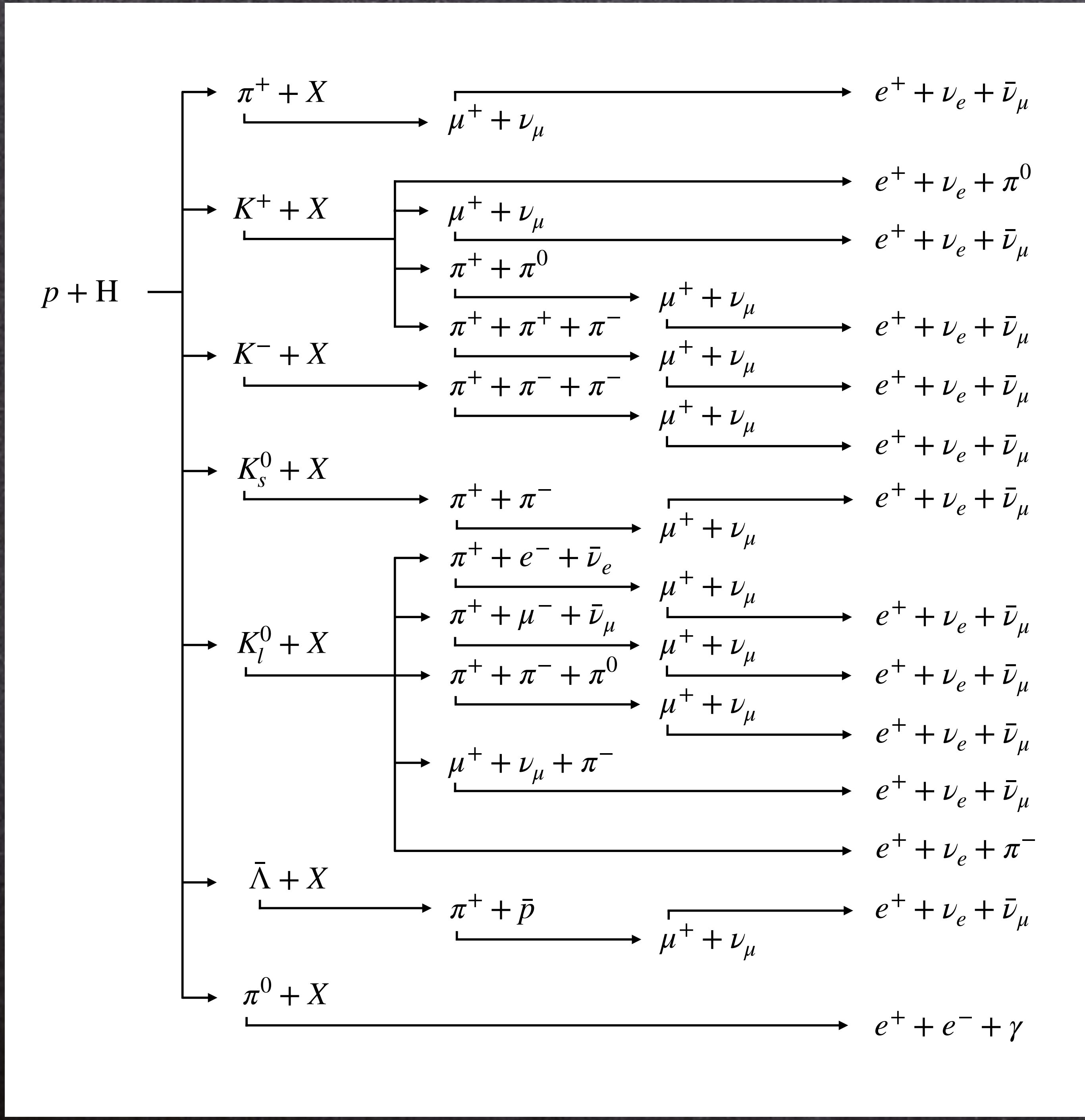

We include all these contributions.

Similarly for collisions with nuclei.

We repeat ALL the analysis for e- under charge conjugation

The e± production chain from π± production

$$\frac{d\sigma_{ij}}{dT_{e^+}}(T_i, T_{e^+}) = \int dT_{\pi^+} \frac{d\sigma_{ij}}{dT_{\pi^+}}(T_i, T_{\pi^+})\, P(T_{\pi^+}, T_{e^+})$$

Integral over the pion production cross section convolved with the probability density function P

$$\frac{d\sigma_{ij}}{dT_{\pi^+}}(T_i, T_{\pi^+}) = p_{\pi^+} \int d\Omega\, \sigma_{\rm inv}^{(ij)}(T_i, T_{\pi^+}, \theta)$$

The pion production cross section is the integral of the Lorentz Invariant cross section over scattering angle (or p_T)

$$\sigma_{\rm inv}^{(ij)} = E_{\pi^+} \frac{d^3\sigma_{ij}}{dp^3_{\pi^+}}$$

The role of secondaries

M. Di Mauro, FD, S. Manconi PRD 2021

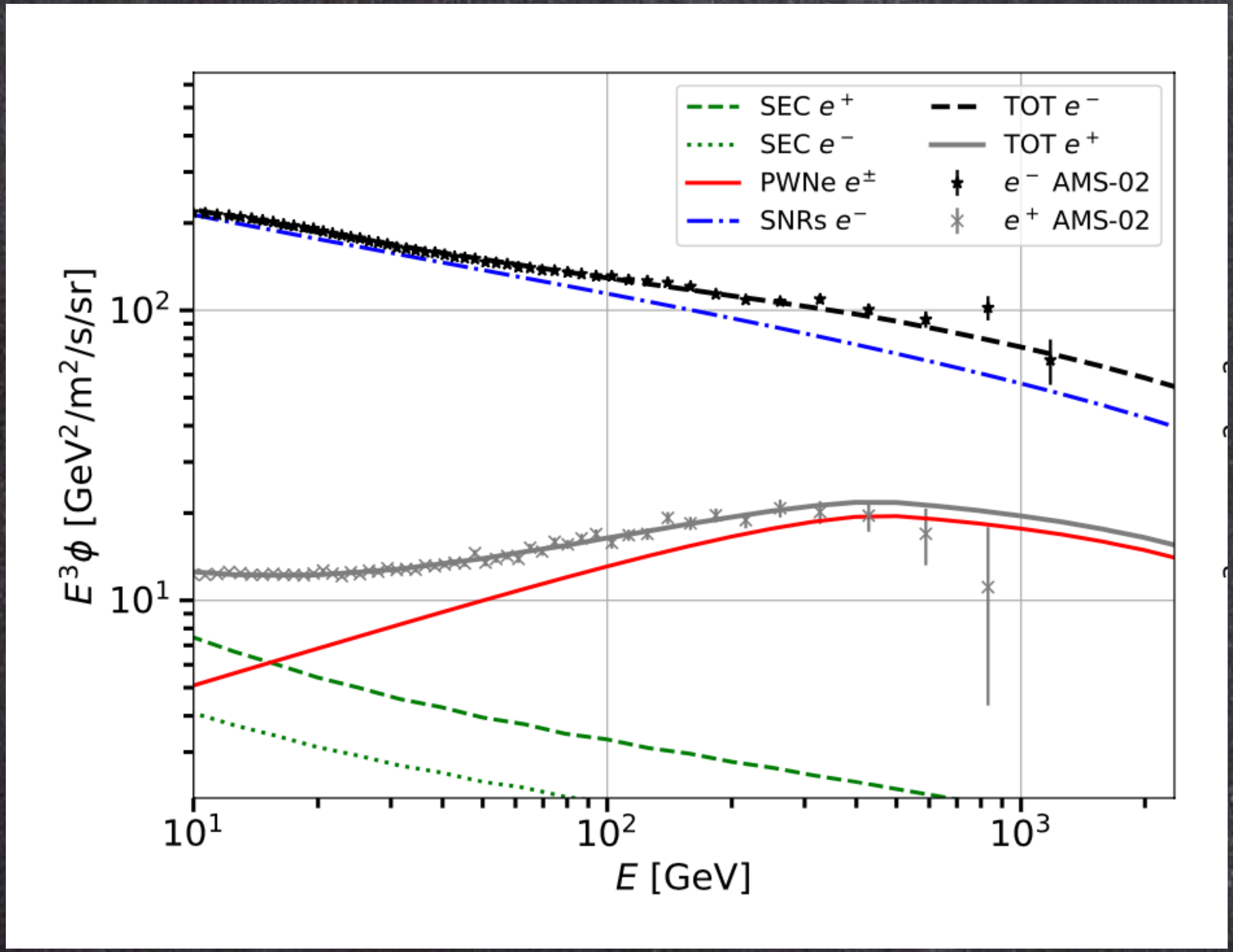

Di Mauro+ JCAP 2014

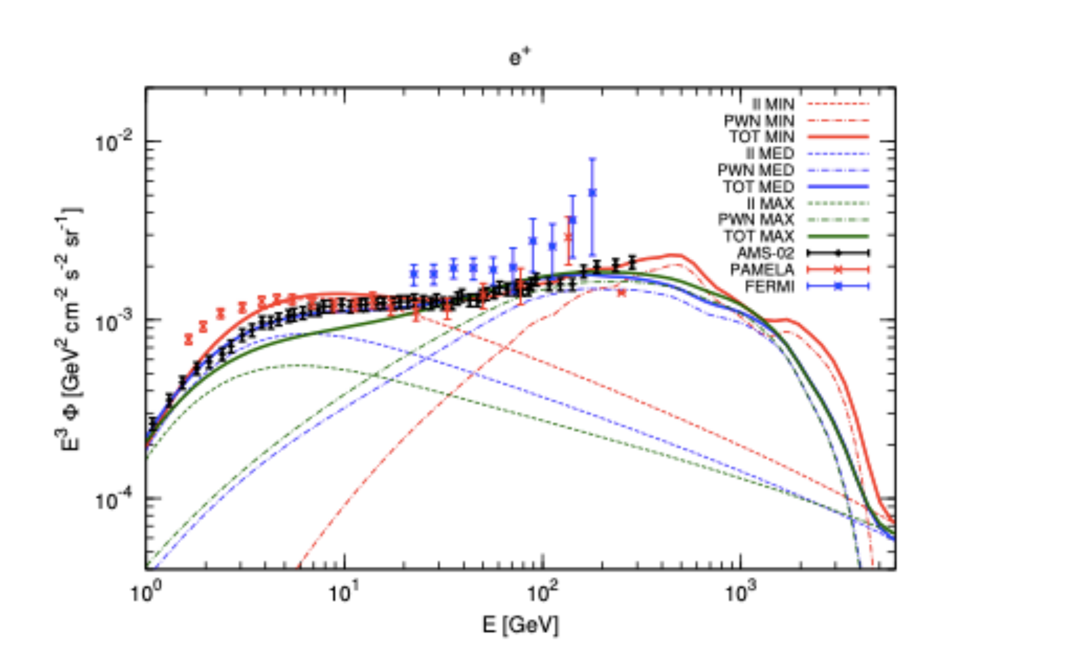

See also Lavalle, Maurin, Putze PRD 2014

e+ secondaries contribute significantly to shape the spectrum at Earth.

The flux in the GeV region is likely dominated by secondaries

An example: Fit of Galactic pulsar populations to AMS-02 e+ data

L. Orusa, FD, M. Di Mauro, S. Manconi, JCAP 2021

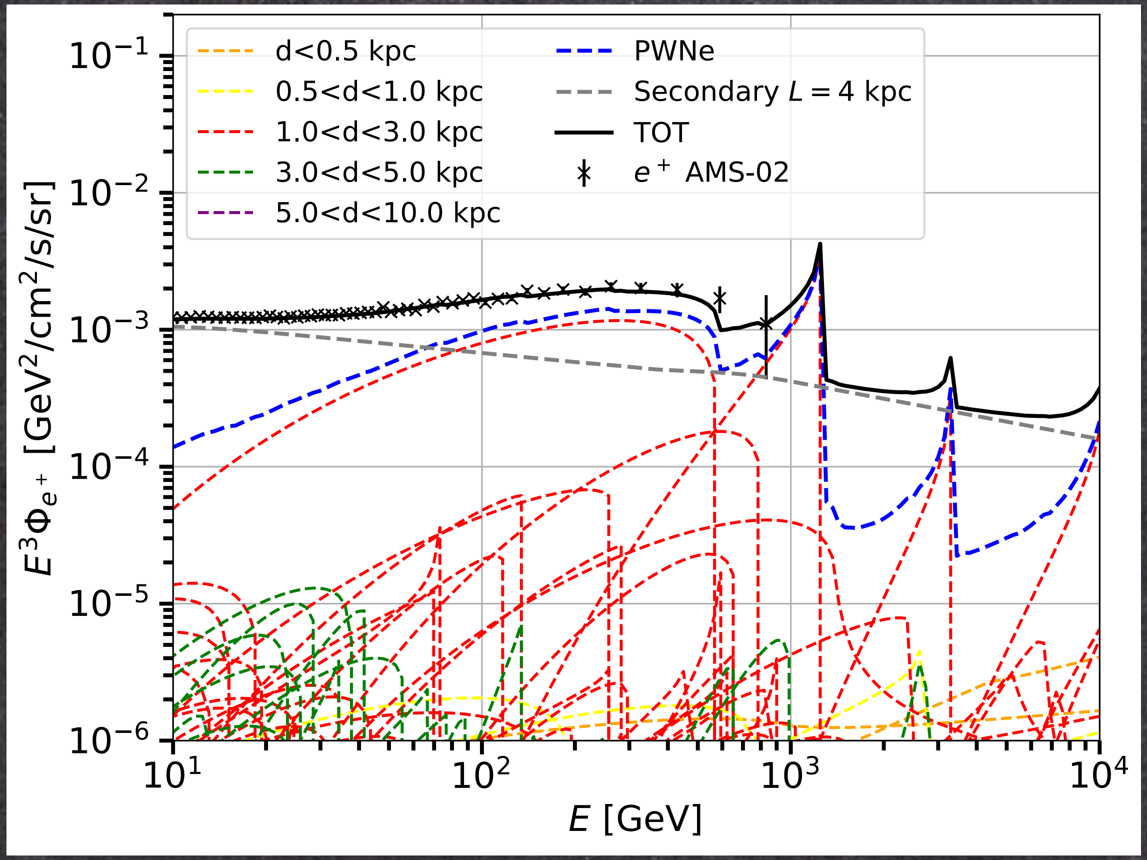

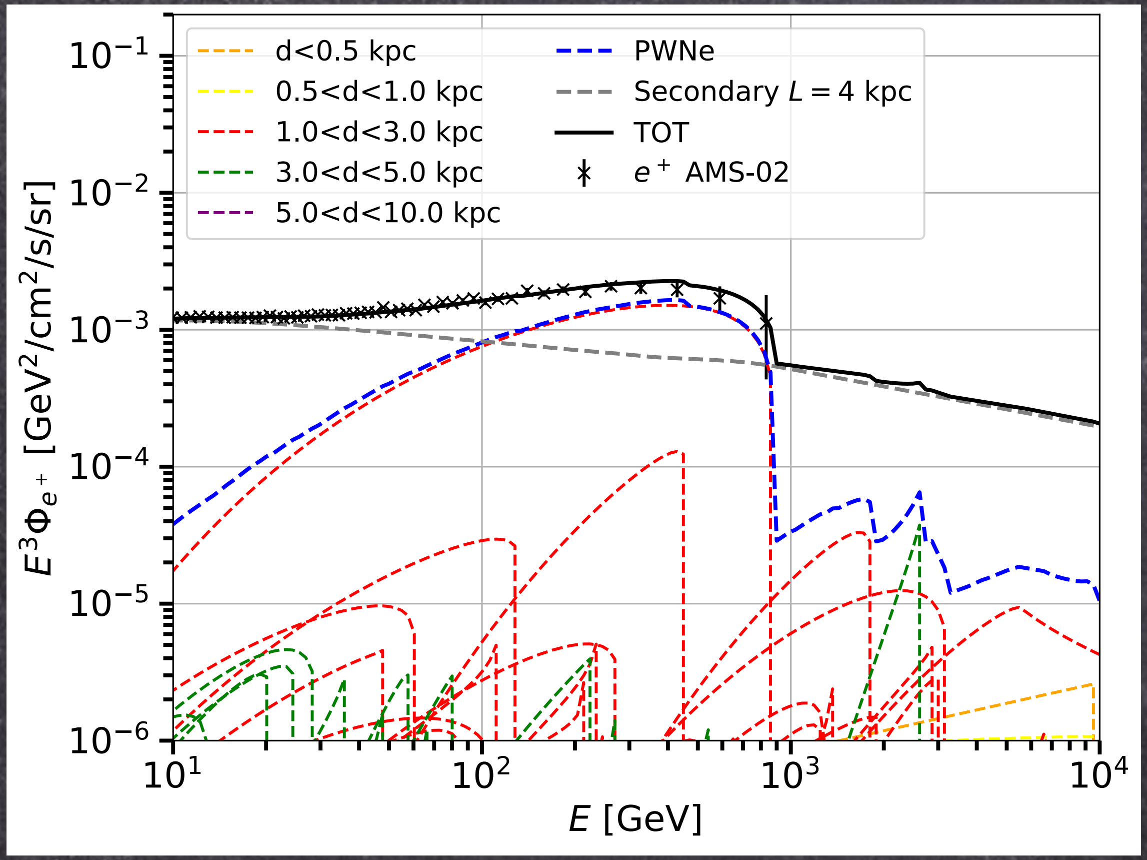

The contribution of pulsars to e+ is dominant above 100 GeV and may have different features. For E>1 TeV: unconstrained by data.

Secondaries forbid evidence of sharp cut-off.

Secondaries are fitted with a free normalization always exceeding 2.

A fit is performed on the σ_{inv} data

L. Orusa, M. Di Mauro, FD, M. Korsmeier, PRD 2022

Experiment	$\sqrt{s}$ [GeV]	$\sigma_{\rm inv}$	n	Ref.
NA49	17.3	×	×	[22]
ALICE	900	×	-	[23]
CMS	900, 2760, 7000, 13000	×	-	[24, 25]
Antinucci	π^+ (3.0, 3.5, 4.9, 5.0, 6.1, 6.8)	-	×	[26]
	π^-(3.0, 3.5, 4.9, 5.0, 6.1, 6.8)	-	×	[26]
	K^+ (2.8, 3.0,3.2, 5.0, 6.1, 6.8)	-	×	[26]
	K^- (4.9, 5.0, 6.1, 6.8)	-	×	[26]
NA61	6.3, 7.7, 8.8, 12.3, 17.3	-	×	[21]

We use data on σ_{inv}, the multiplicity n or both.

The NA49 data

C. Alt et al., Eur. Phys. J. C, 2005

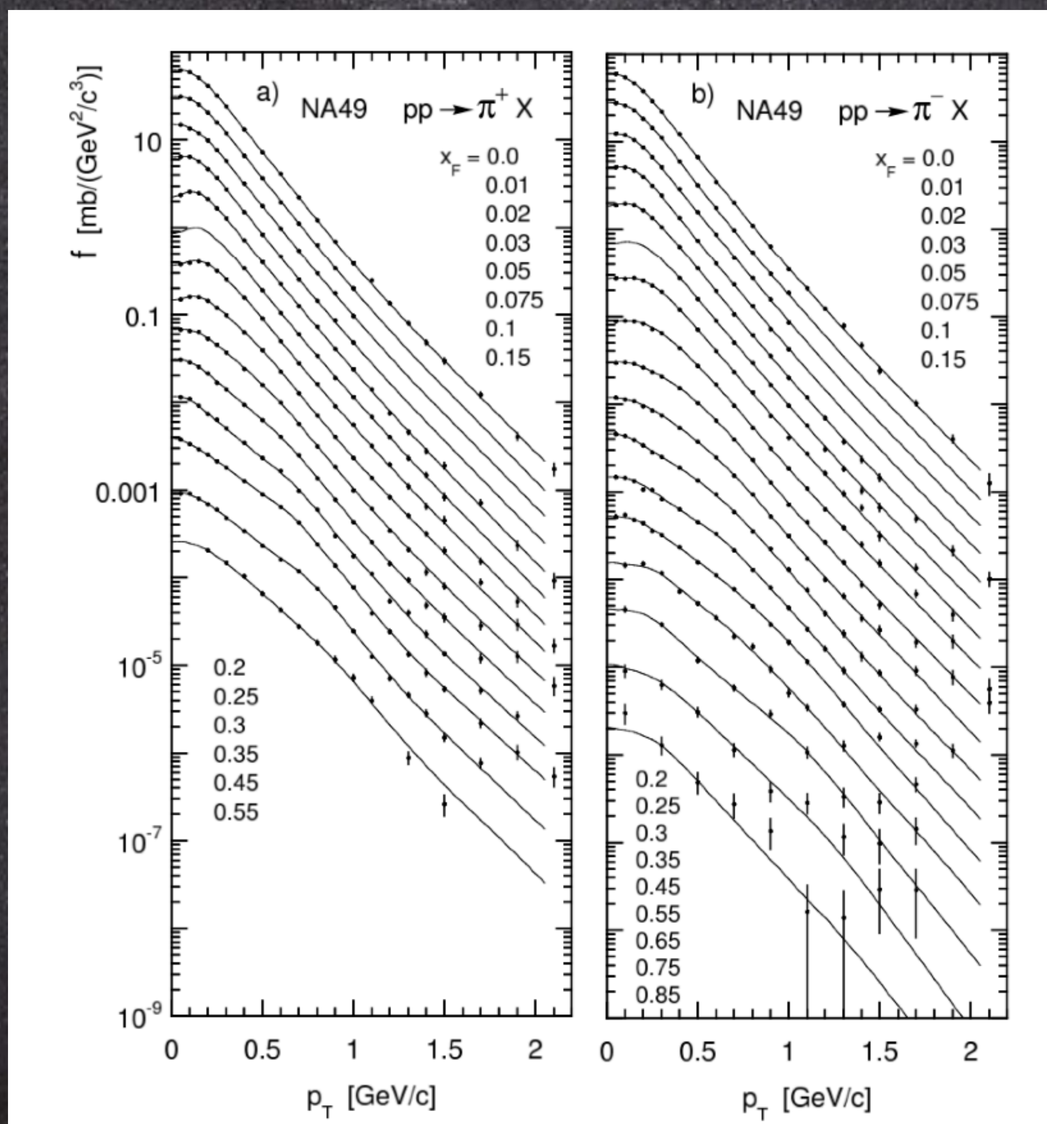

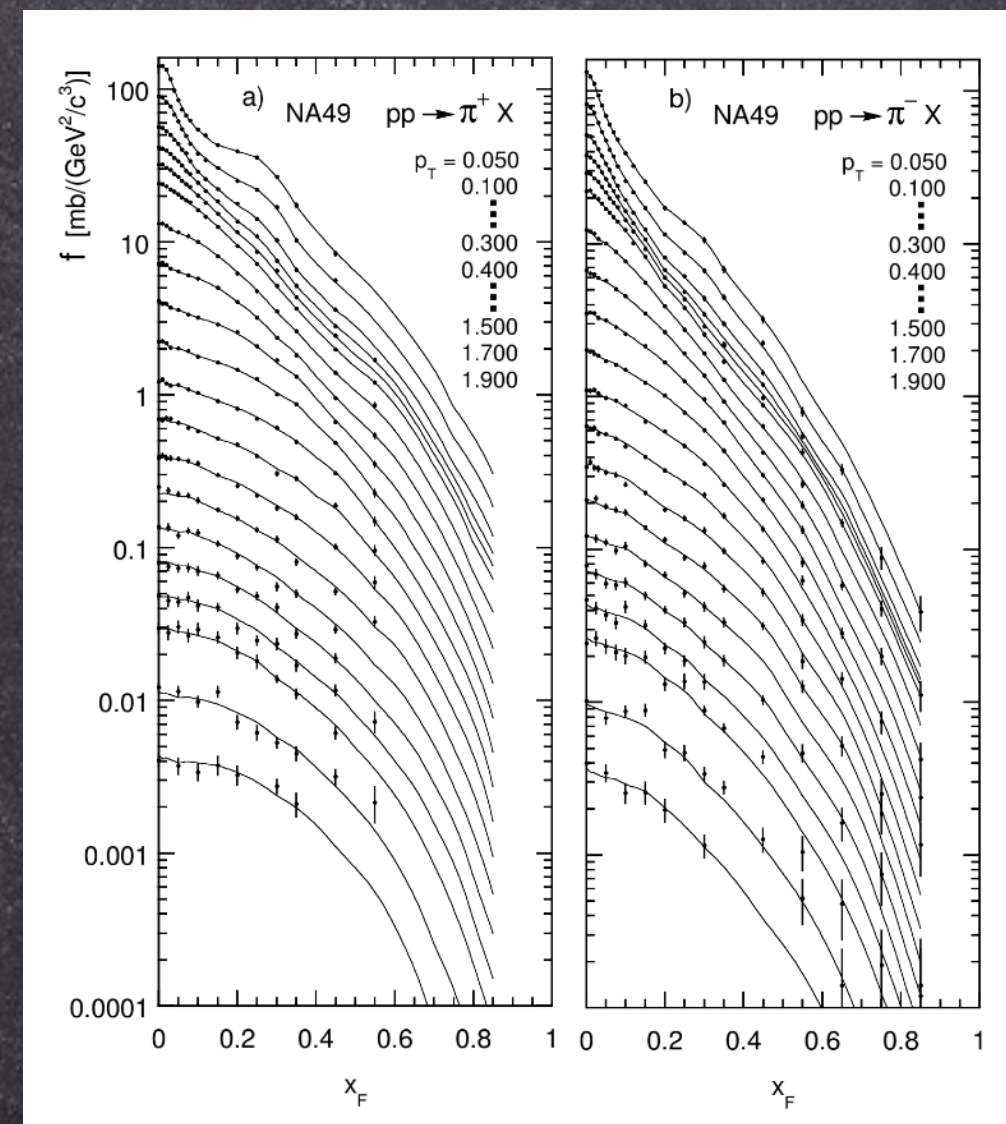

Wide ranges in p_T and x_F are covered at E_p=158 GeV

Data correction for feed-down

The pion production cross section can contain (or not) the pions from weak decays of strange particles.

C. Alt et al., Eur. Phys. J. C, 2005

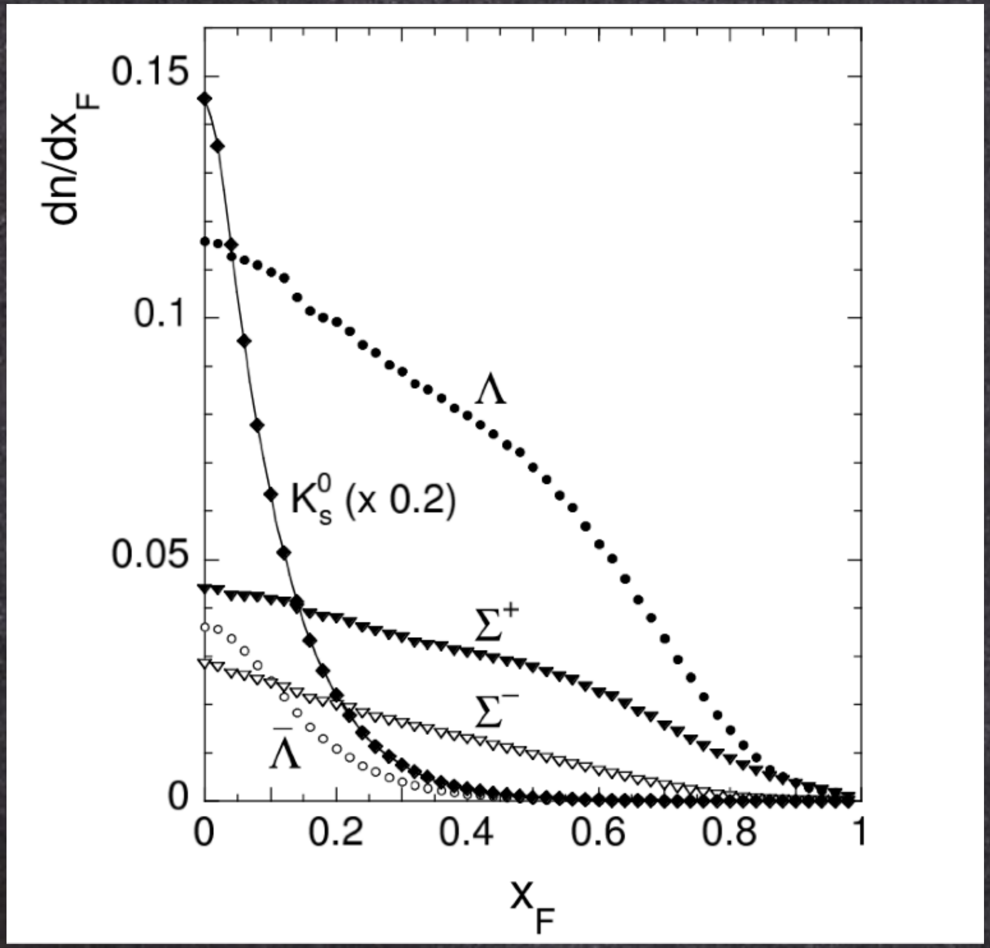

NA49 p_T integrated, MC

Almost all the data except the older ones are feed-down corrected.

When not, we correct for it.

Results on the σ_{inv} for π^+ production: NA49

L. Orusa, M. Di Mauro, FD, M. Korsmeier, PRD 2022

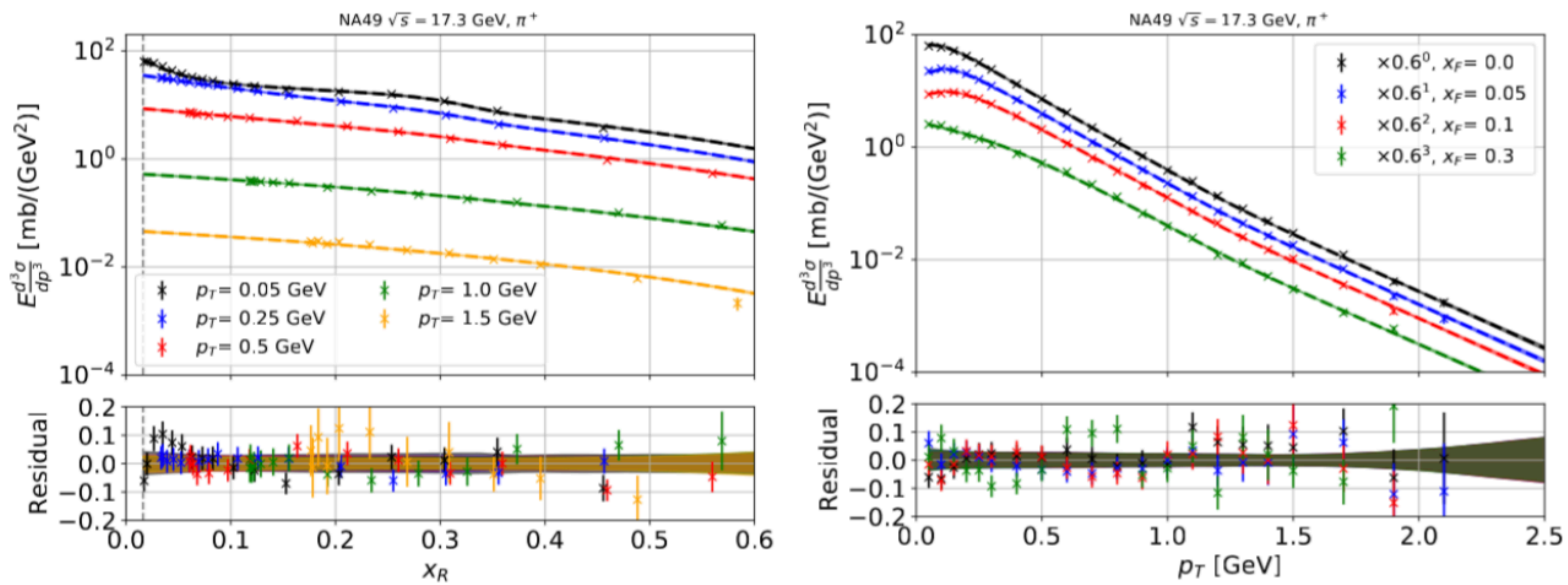

FIG. 2. Results of the fit on the NA49 data [22] invariant cross section for the inclusive π^+ production in $p+p$ collisions. On the left (right) plot we show the NA49 data along with our fit results for representative values of $p_T = 0.05, 0.25, 0.5, 1.0, 1.5$ GeV ($x_F = 0.0, 0.05, 0.2, 0.3$) values, as a function of x_R (p_T). For clarity in the right plot, each curve and data have been multiplied by a factor of $0.6^{n_{x_F}}$, where n_{x_F} is the integer ($n = 0, 1, 2, ...$) counting the x_F from lower to higher (i.e. for $x_F = 0.1$ the rescaling is 0.6^2). Each curve is plotted along with its 1σ C.L. uncertainty band. In the bottom part of each panel we plot the residuals, which are defined as (data-model)/model, and the width of the 1σ C.L. uncertainty band on the model.

Data are fitted with very small uncertainties

Our parameterisations are appropriate, data are very precise

Results on different sqrt(s)

L. Orusa, M. Di Mauro, FD, M. Korsmeier, PRD 2022

We use σ_{inv} or multiplicity

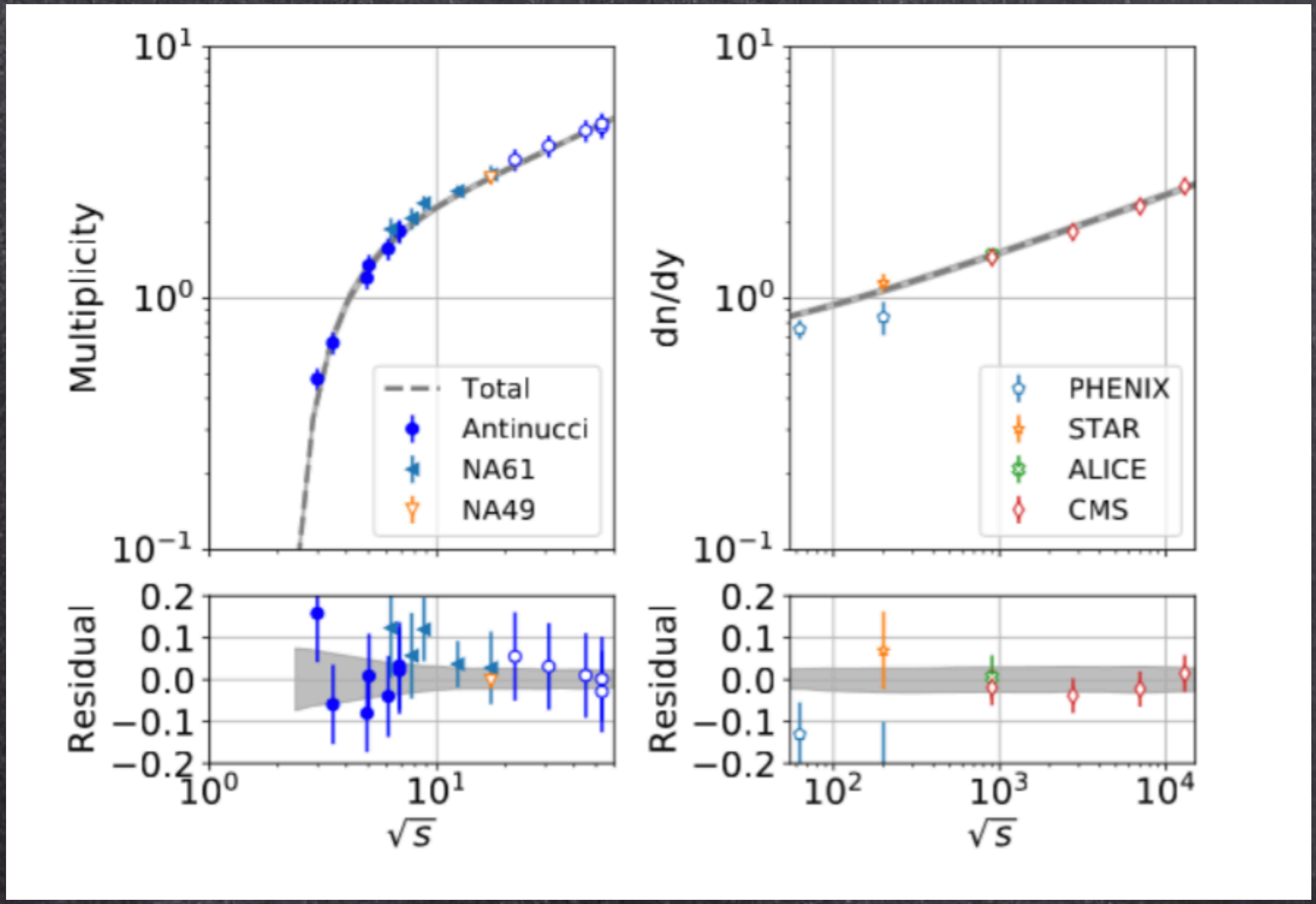

The multiplicity is reproduced as a function of sqrt(s)

The differential cross section for the production of e+ from p+p—>π^++X

L. Orusa, M. Di Mauro, FD, M. Korsmeier, PRD 2022

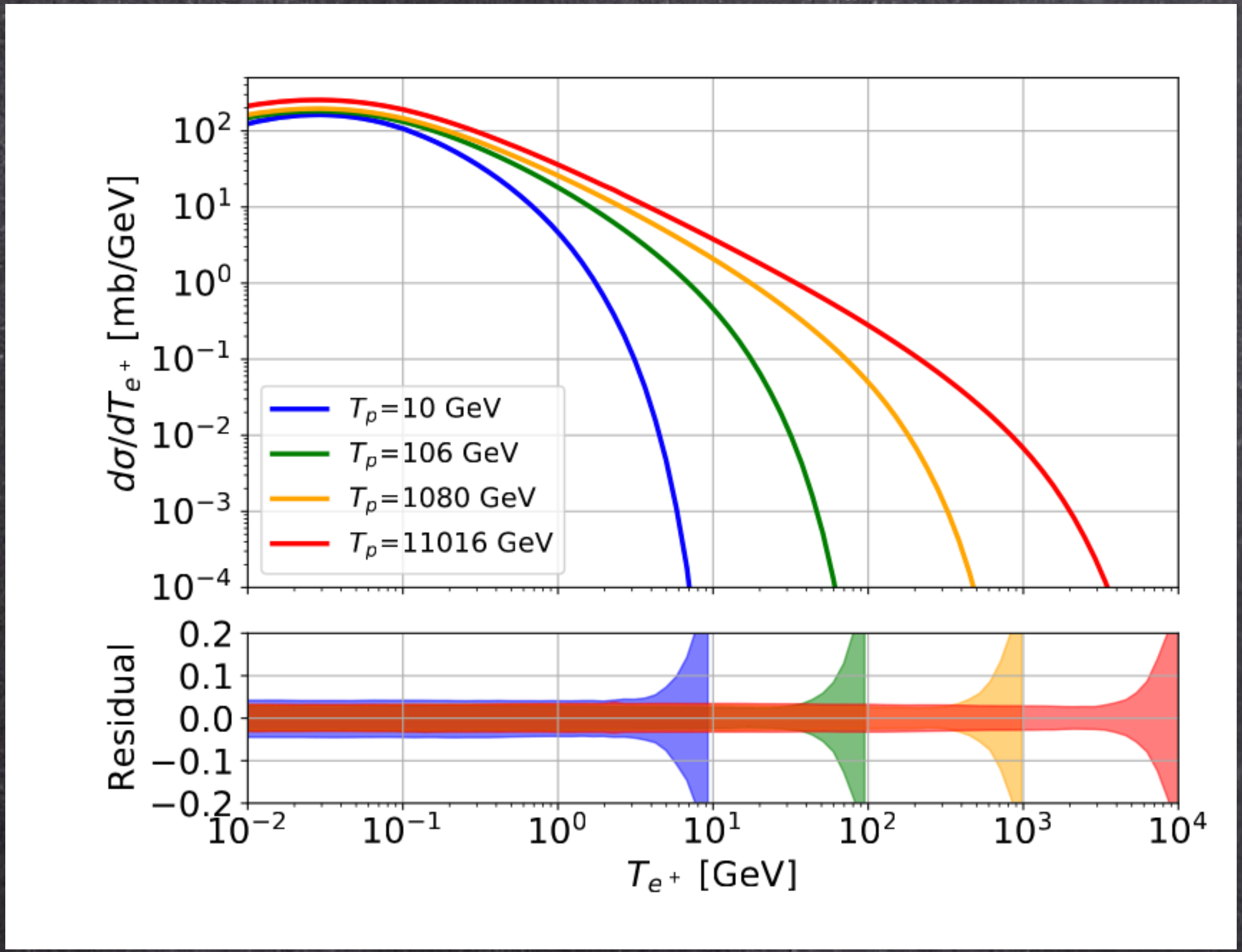

Differential cross section for given incident beam T_p energy.
It is extremely well defined for most of the phase space

Contribution from p+p→K⁺+X

L. Orusa, M. Di Mauro, FD, M. Korsmeier, to appear

Kaons are produced about 10 times less than pions.
We repeat the same fit procedure as for π^+.

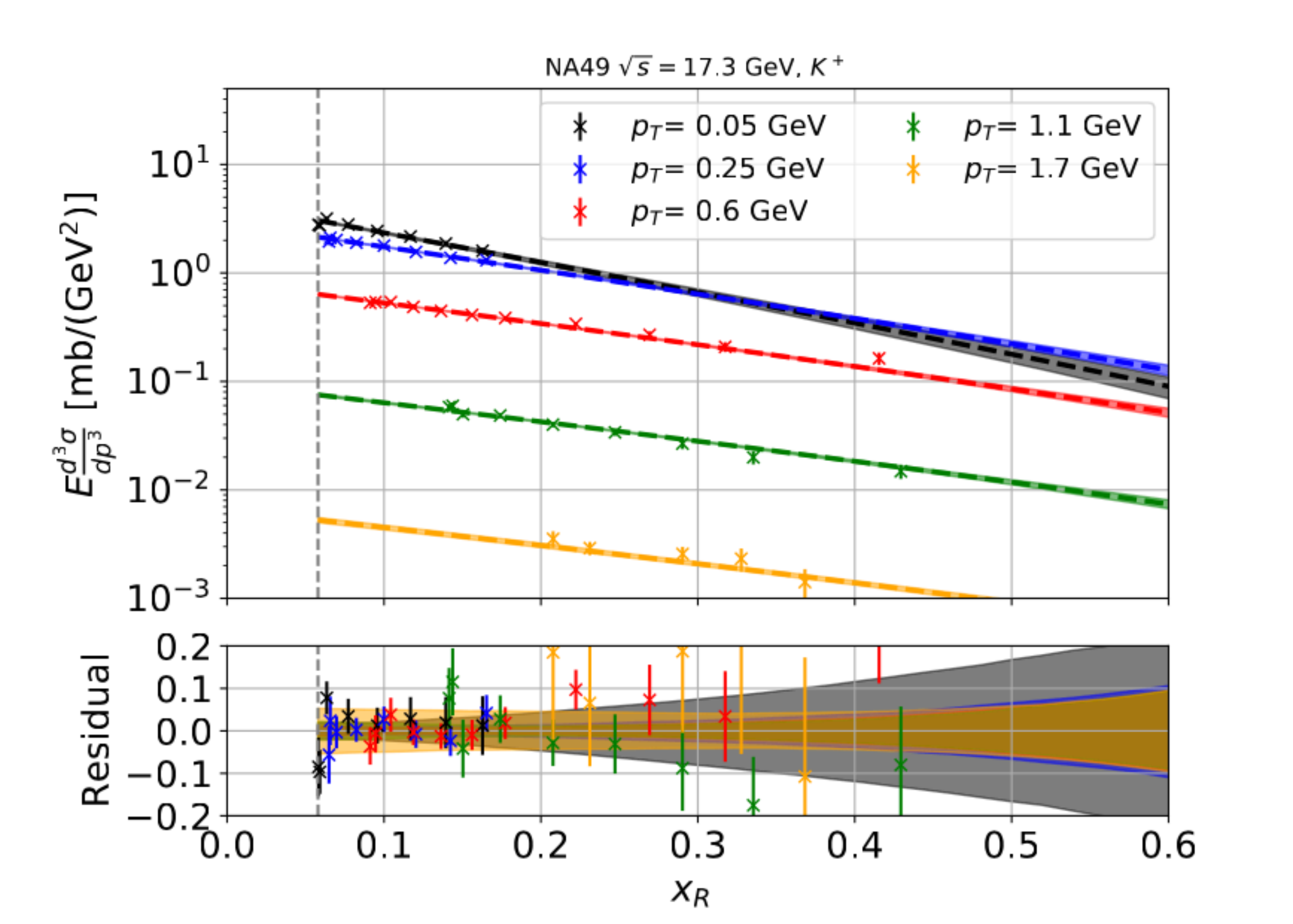

Uncertainty increases with x_R

Production cross section for e+

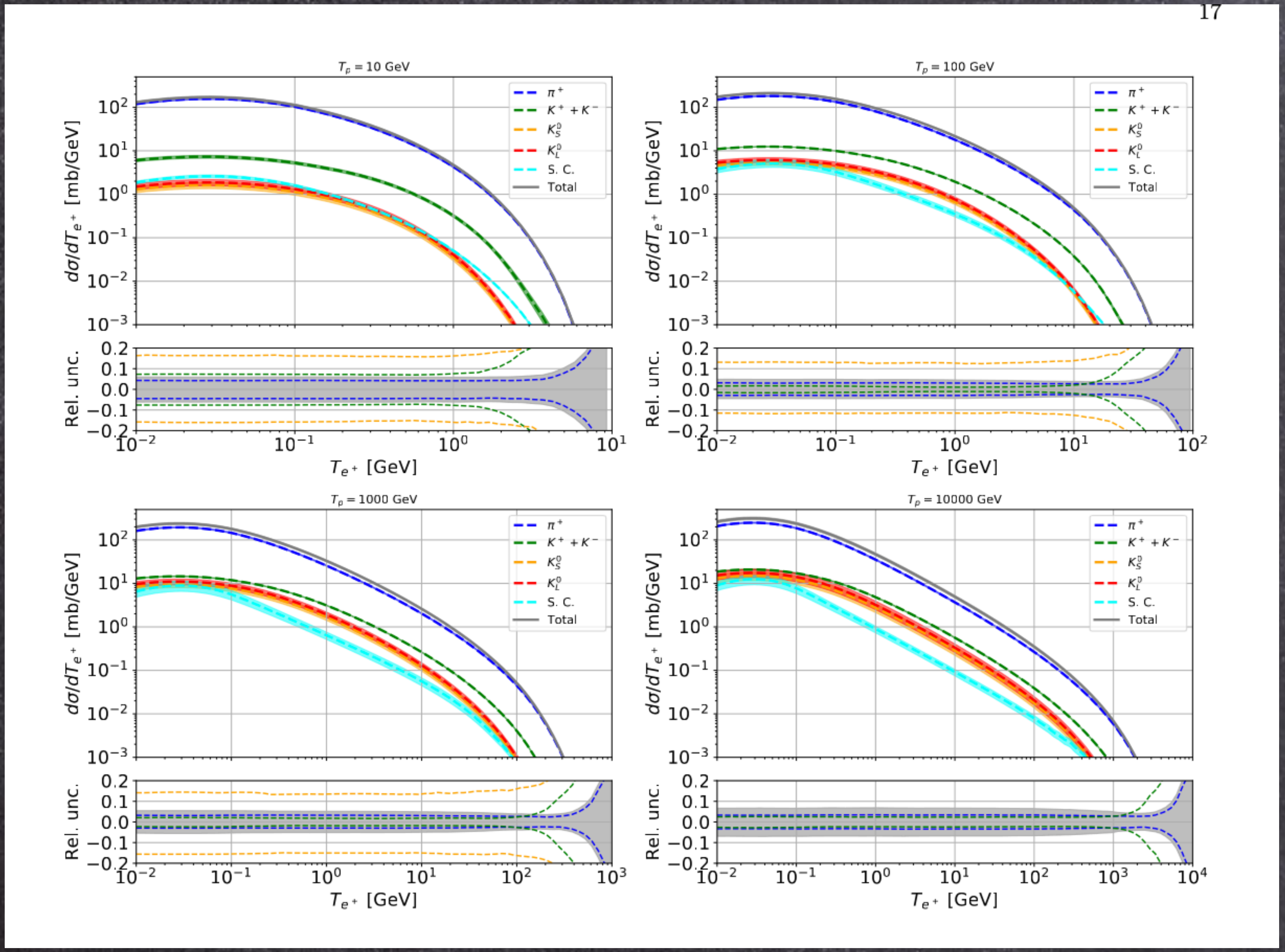

We have computed all the O(1%) contributions

Uncertainty on cross sections is now moderate

The source spectrum

A convolution with CR nuclei and the density of the interstellar medium

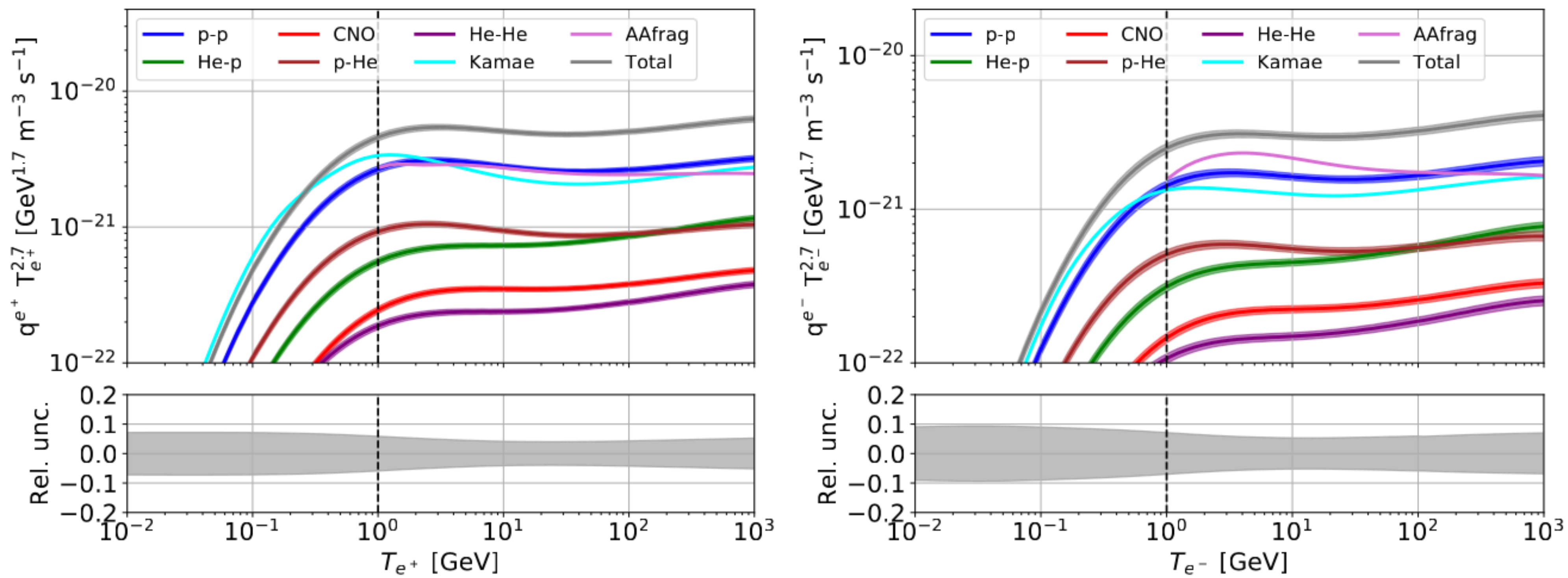

FIG. 13. Source terms of CR e^+ (left panel) and e^- (right panel). Next to the total source term we show the separate CR-ISM contributions. In the bottom panels, we display the relative uncertainty of the total source term. We note, however, that for $T_{e^+} \lesssim 1$ GeV (black dashed line) the source term is not constrained by cross section data but rather an extrapolation of our parametrization which could possibly be affected by systematics.

Uncertainties reduced from a factor 2 to 6-7 %

The photon count composition

Emission of gamma-rays is predicted from:

- The Galactic gas (HI, HII, DNG): π^0 decay
- A Galactic Inverse Compton (IC) photon population
- An isotropic (mostly extragalactic) background

- Point sources
- Extended sources (included Fermi Bubbles and Loop I)
- Sun and Moon
- Residual Earth Limb (negligible for $E > 200$ MeV)
- Diffuse emission from Dark Matter annihilation

The Fermi-LAT diffuse γ-ray emission of the Galaxy dominates over point sources (x 5 at $E > 50$ MeV), 50% from latitudes $|b|<6°$

A hot case: Hadronic photon production

Orusa, Di Mauro, Donato, Korsmeier in progress

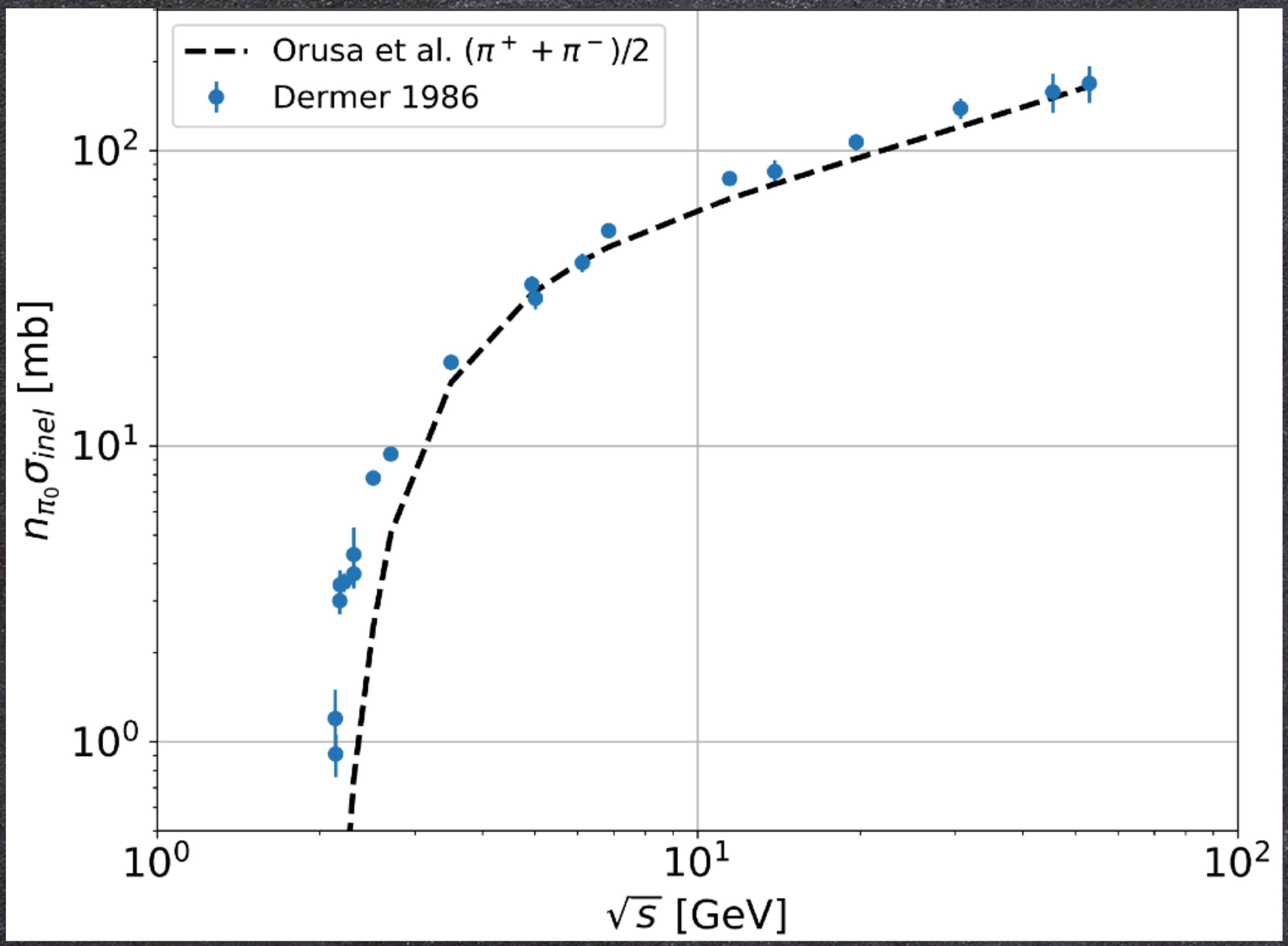

Production of \gamma rays
From p (He) - p(He) scatterings

Determines the intensity of the galactic diffusion emission

Some data on multiplicities

Data on Lorentz invariant cross section almost do NOT exist (true?)

Conclusions

Great efforts to better understand nuclei and antinuclei in CRS: theory models, data from space, data from colliders.

Data from space are actually hampered by lack of precise (<10%) ross section: nuclei, isotopes, antimatter, γs

Data from colliders are highly desirable.
A specific receipt can be provided by the astroparticle community

Interactions and decays in the Galaxy

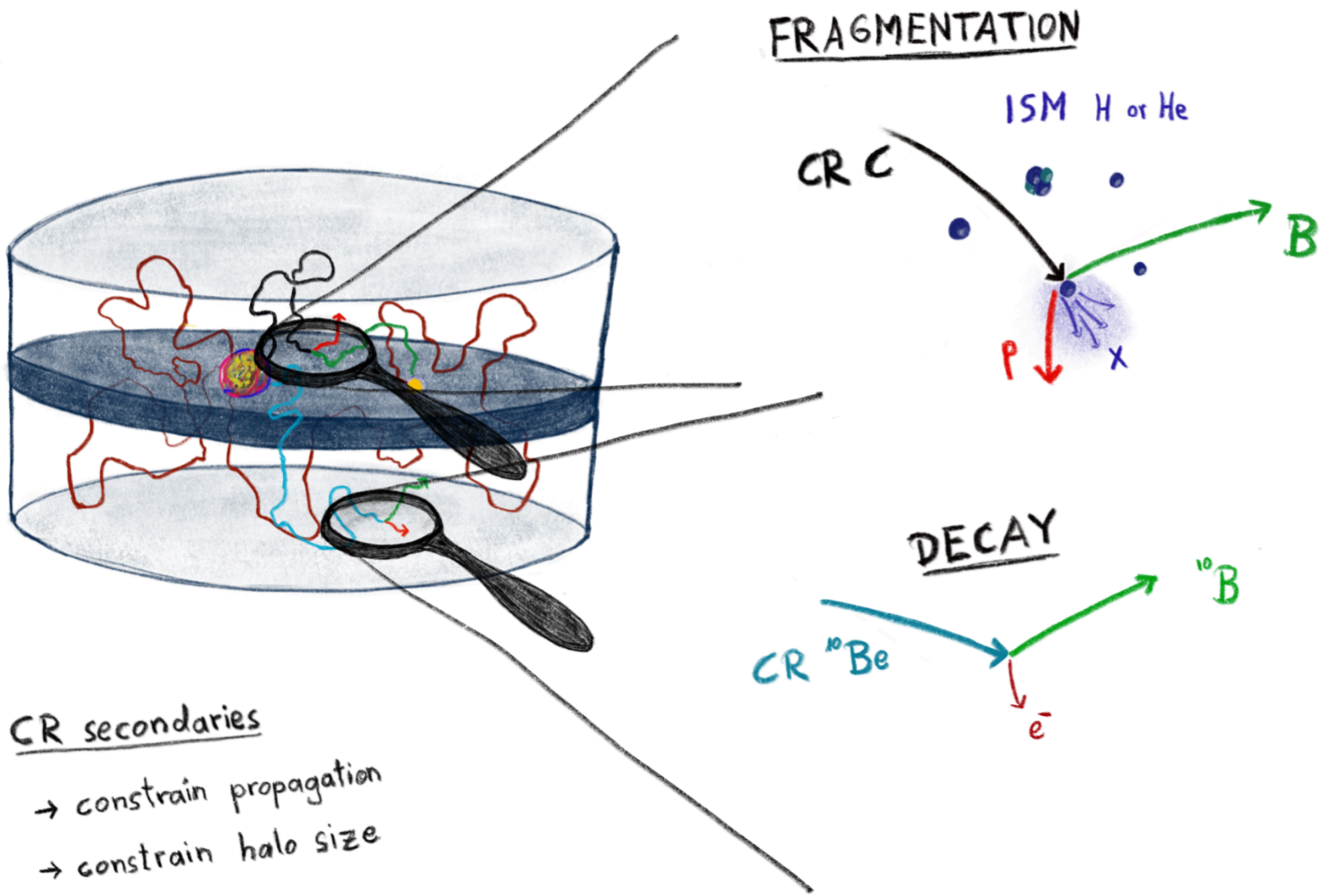

Courtesy of M. Korsmeier

Light isotopes in cosmic rays

Important to test origin and propagation of CRs
Radioactive isotopes can track the diffusive halo size

Derome PoS ICRC 2021

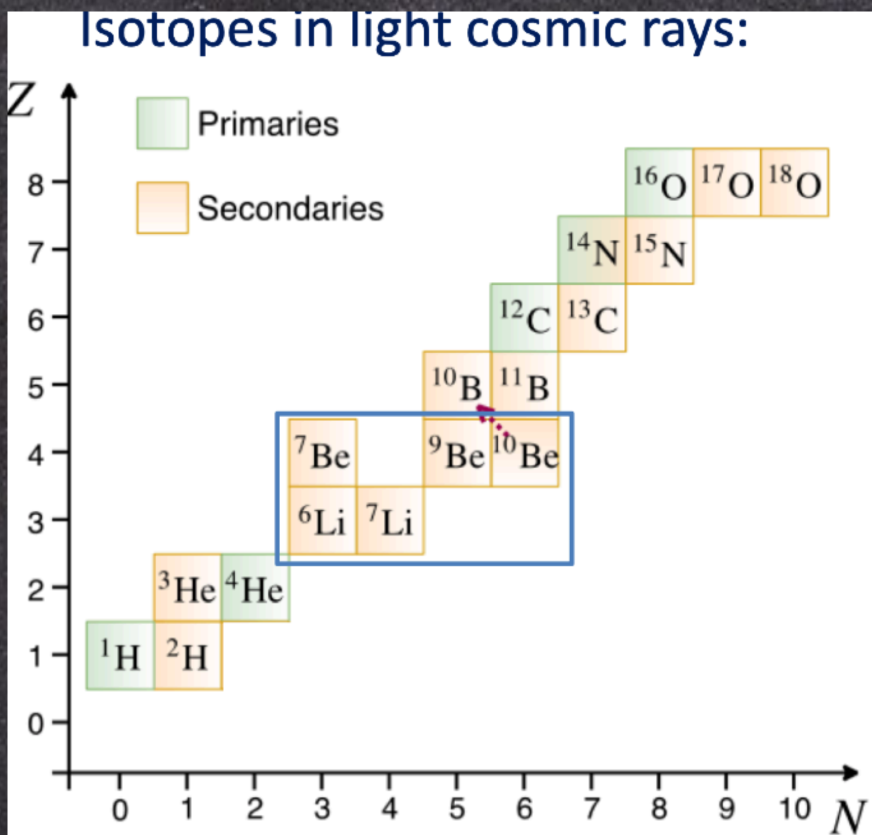

Radioactive isotopes have different propagation history

FD, Maurin, Taillet A&A 2001

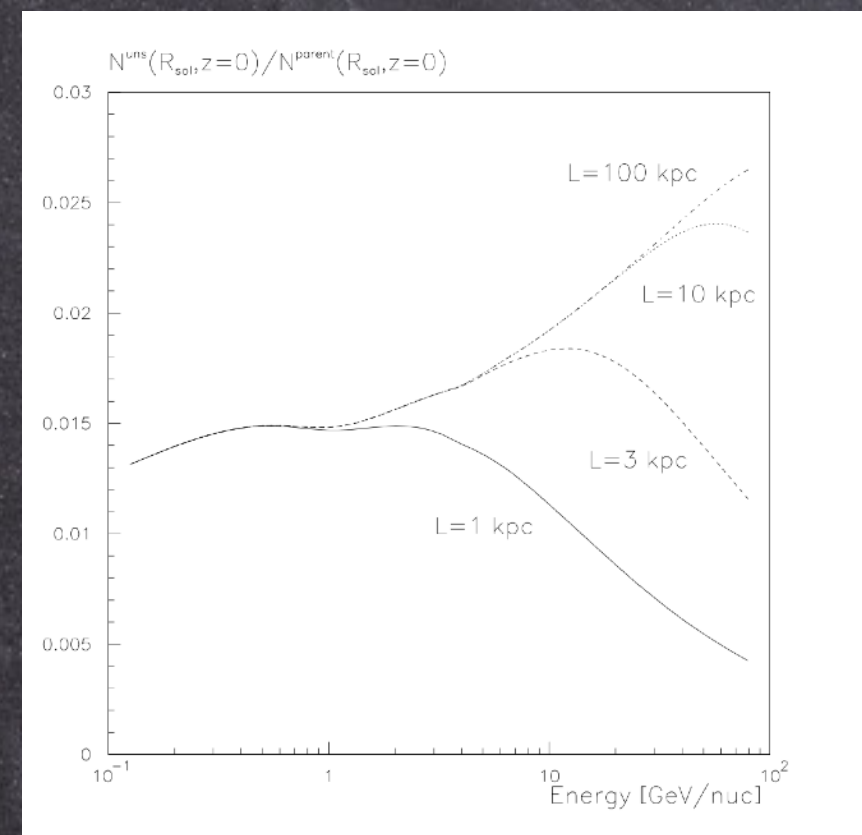

Unstable ^{26}Al to stable ^{28}Si parent ratio

$$l_{rad} = \sqrt{D(E)\gamma\tau_0} < L$$

: insensitive to halo size

Recent results with light nuclei isotopes

L.Derome AMS-02, ICRC 2021 PoS

Weinrich et al. A&A 2020
Maurin et al, 2203.07265

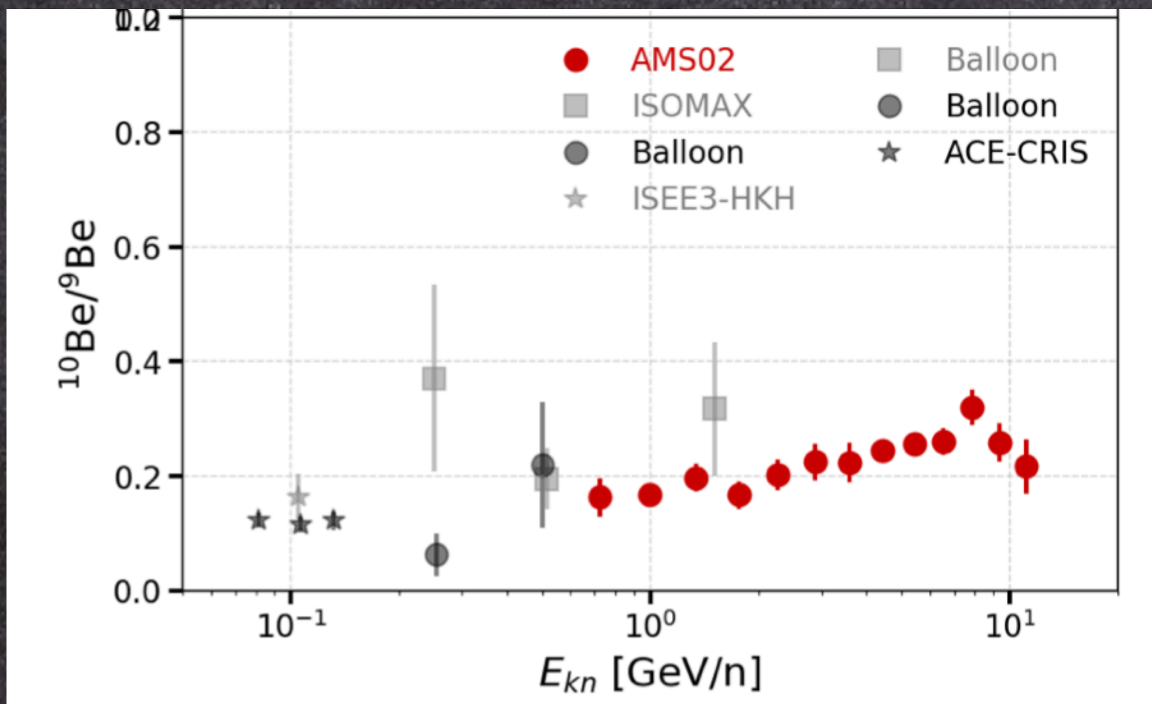

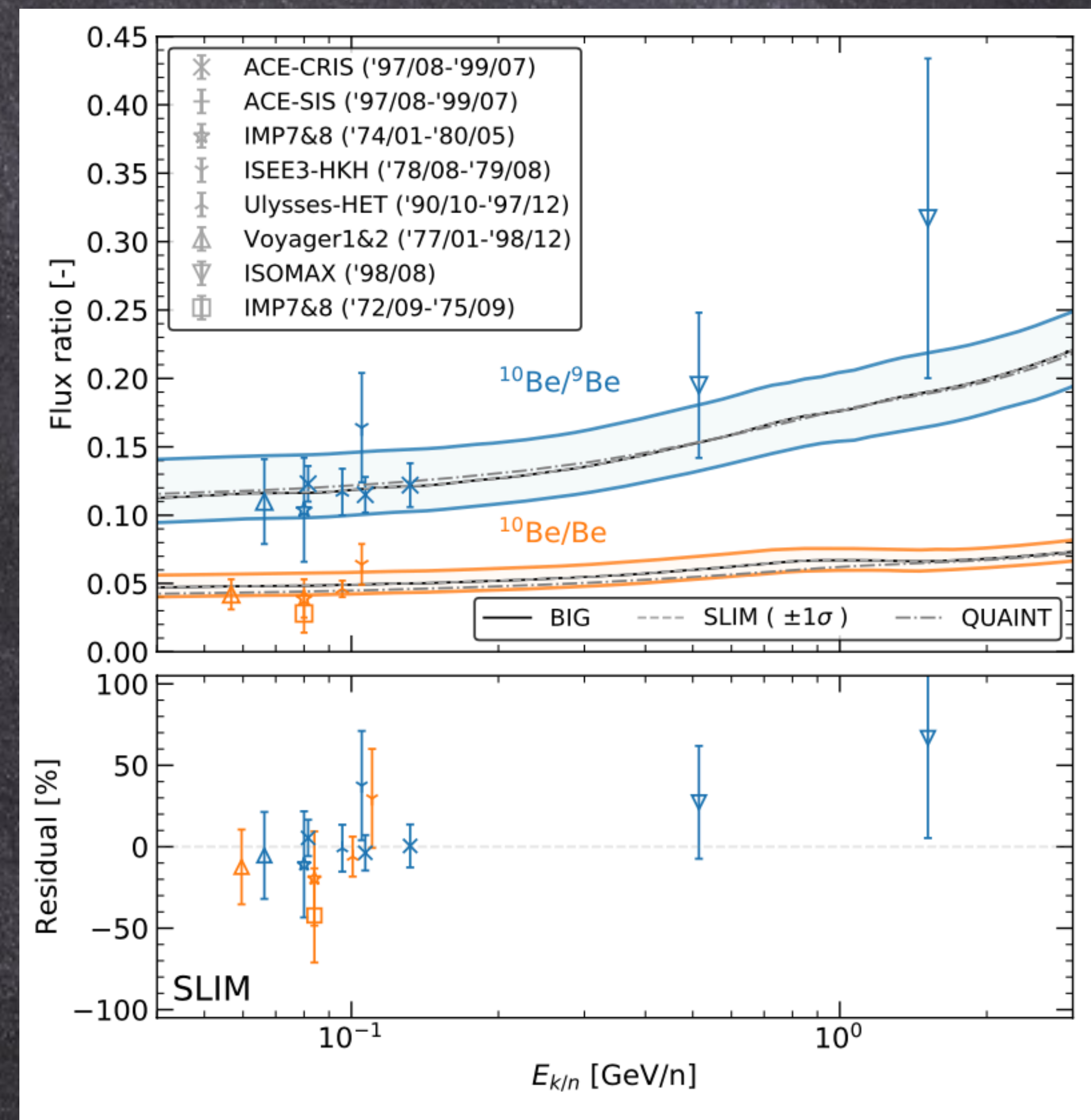

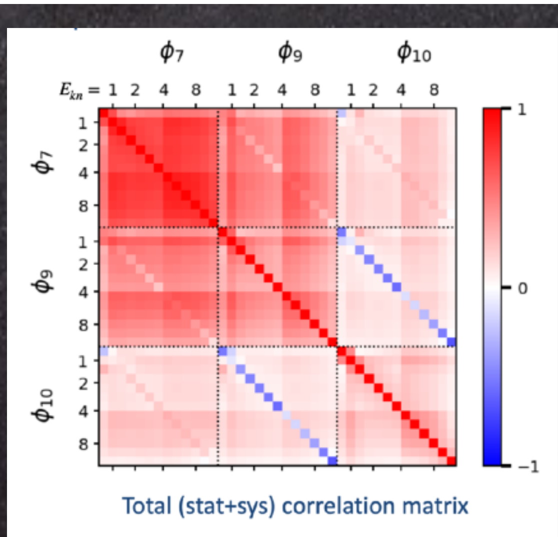

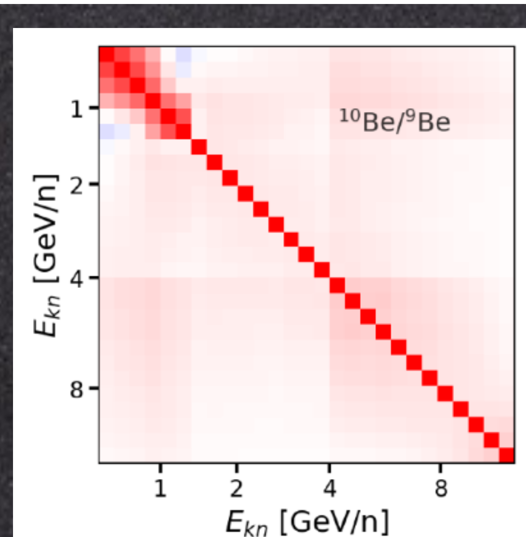

Several isotopes measured up to 10 GeV/n, with correlation matrices

Indications to rather high diffusive halo (>=5 kpc)

Spallation cross sections for nuclei: the F case

Vecchi, Bueno, Derome, Genolini, Maurin PoS ICRC 2021

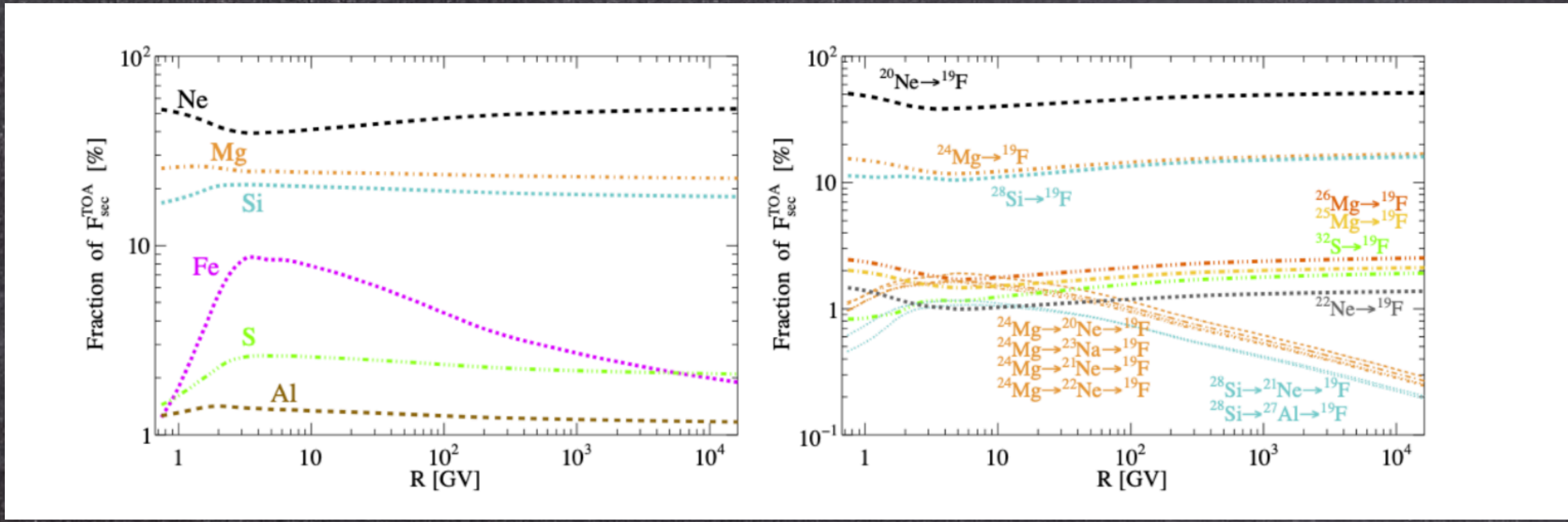

Main progenitors are Ne, Mg, Si, S, Al, and other 35 channels contributing individually [0.1,2]%, 22% of the total.

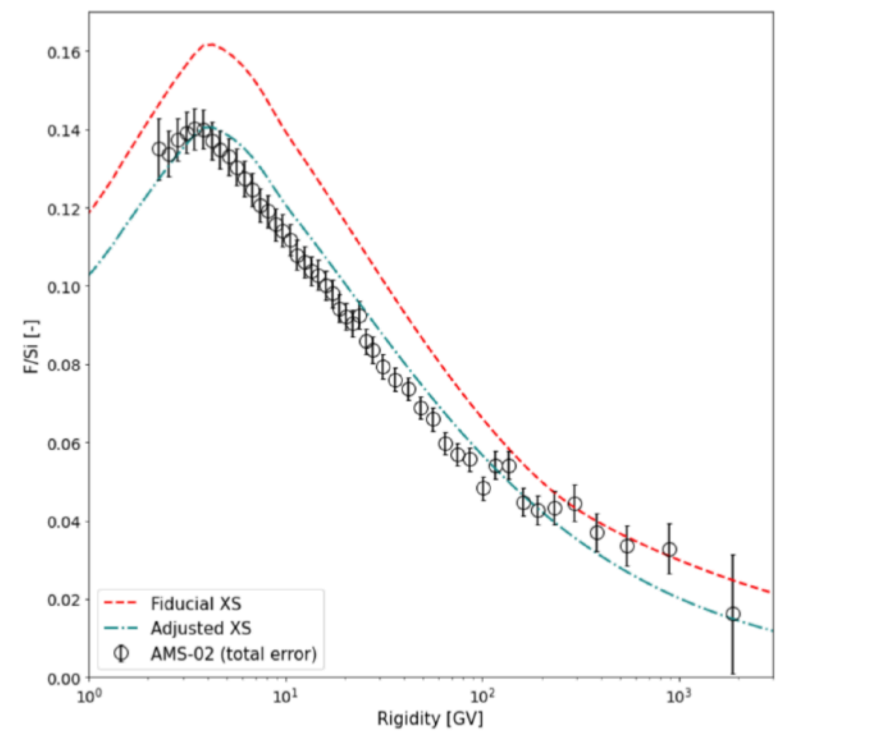

Propagation parameters from lighter nuclei over-predict F/Si.
If cross sections are reduced by 15%, agreement is found for Li to F secondaries

For next generation experiments

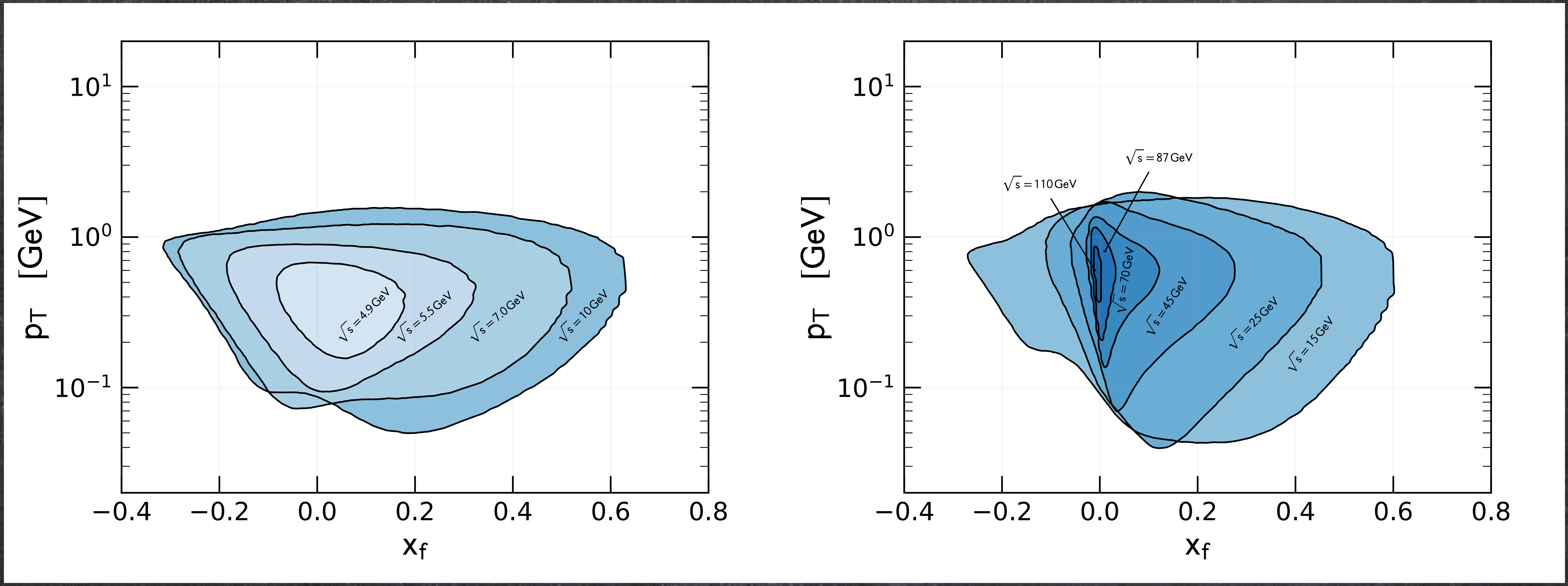

AMS-02 accuracy is reached if pp → pbar cross section is measured with 3% accuracy inside the regions, 30% outside.

Antihelium-3 production

First data at LHC/Alice, Alice Coll. PRC 2018

Data at 0.9, 2.76, 7 TeV sqrt(s)

Invariant yields

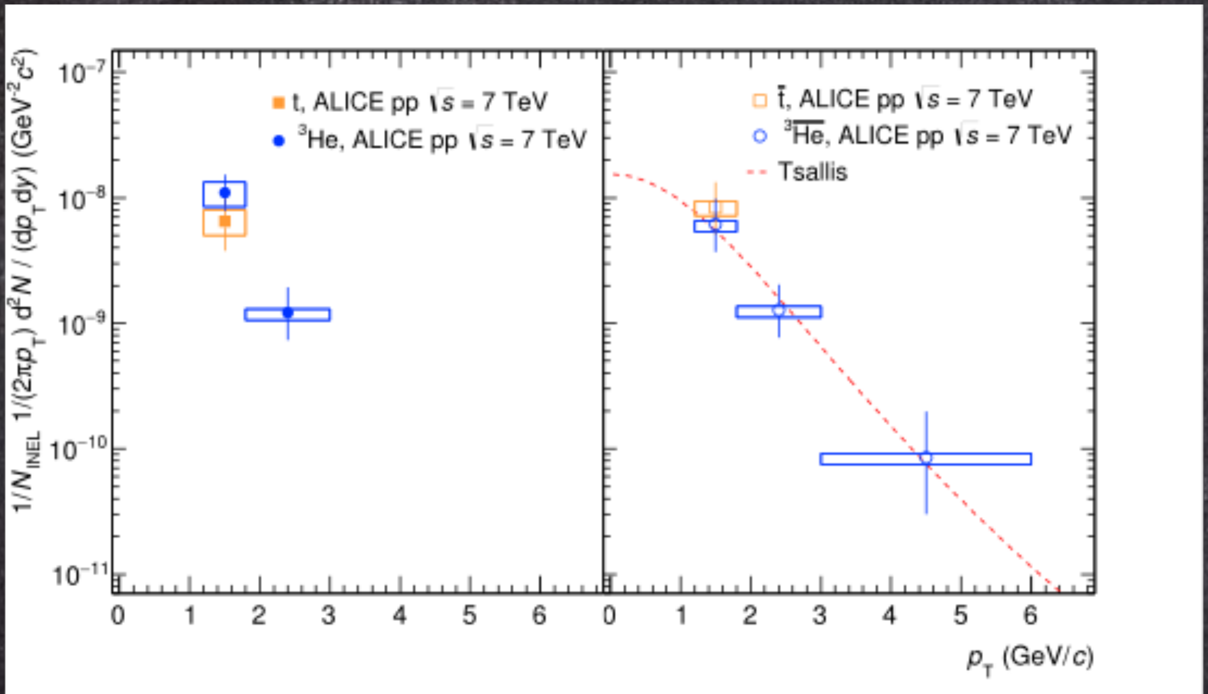

Coalescence parameter

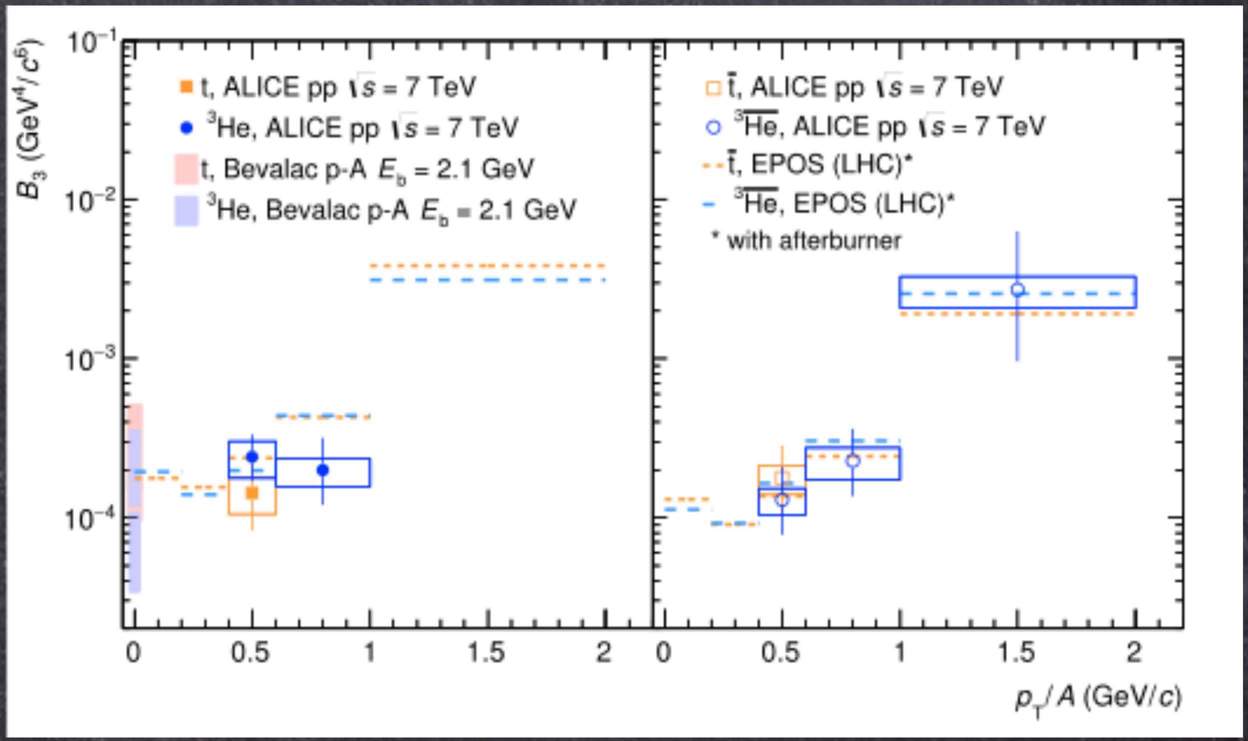

Previous data from Bevalac on ³He, consistent with Alice.

Measured a p_T dependence, but non very relevant in the Galaxy (see inv. yield)

P_{coal} greater (122 MeV vs 98 MeV) than in previous estimations $(p_{coal})^6$

The effect of inelastic cross sections

Serksnyte et al, PRD 2022

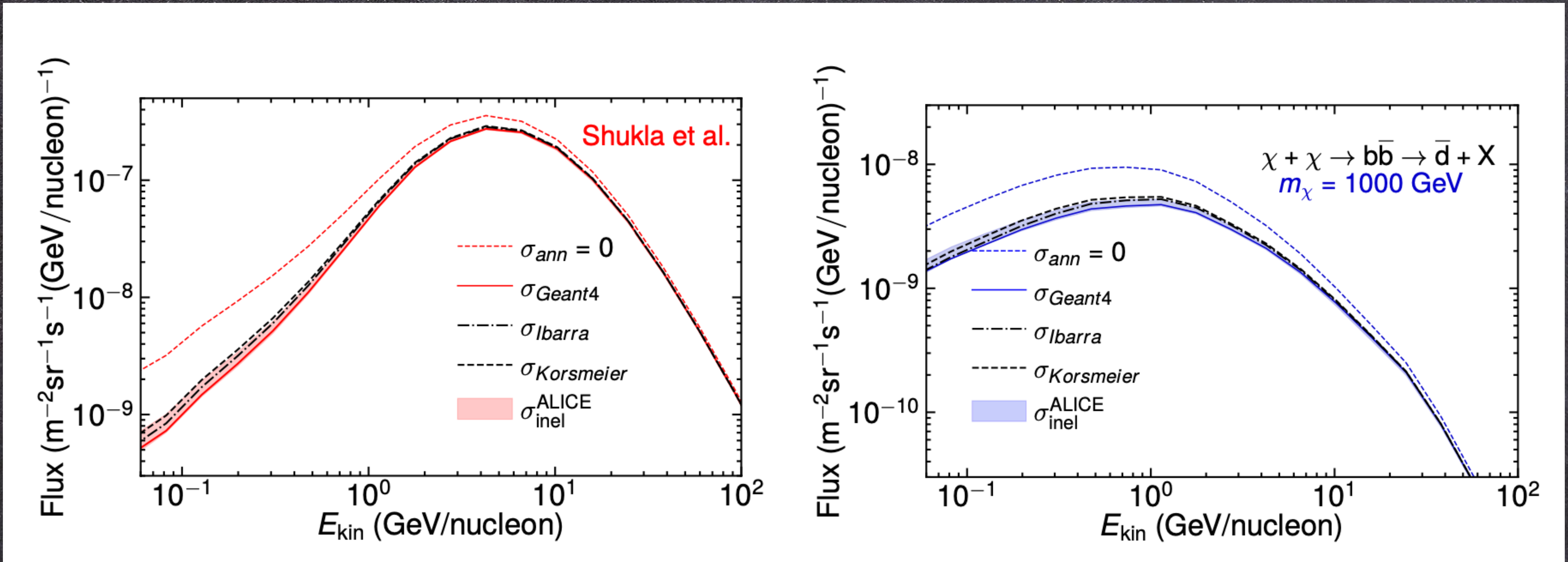

Destruction on the ISM is relevant for sharp spectra (i.e. secondary one), especially in the GAPS energy range. Cross sections are under control

Effect of galactic propagation

Genolini+ PRD 2021

New AMS-02 sec/prim data allow reduction of propagation uncertainties

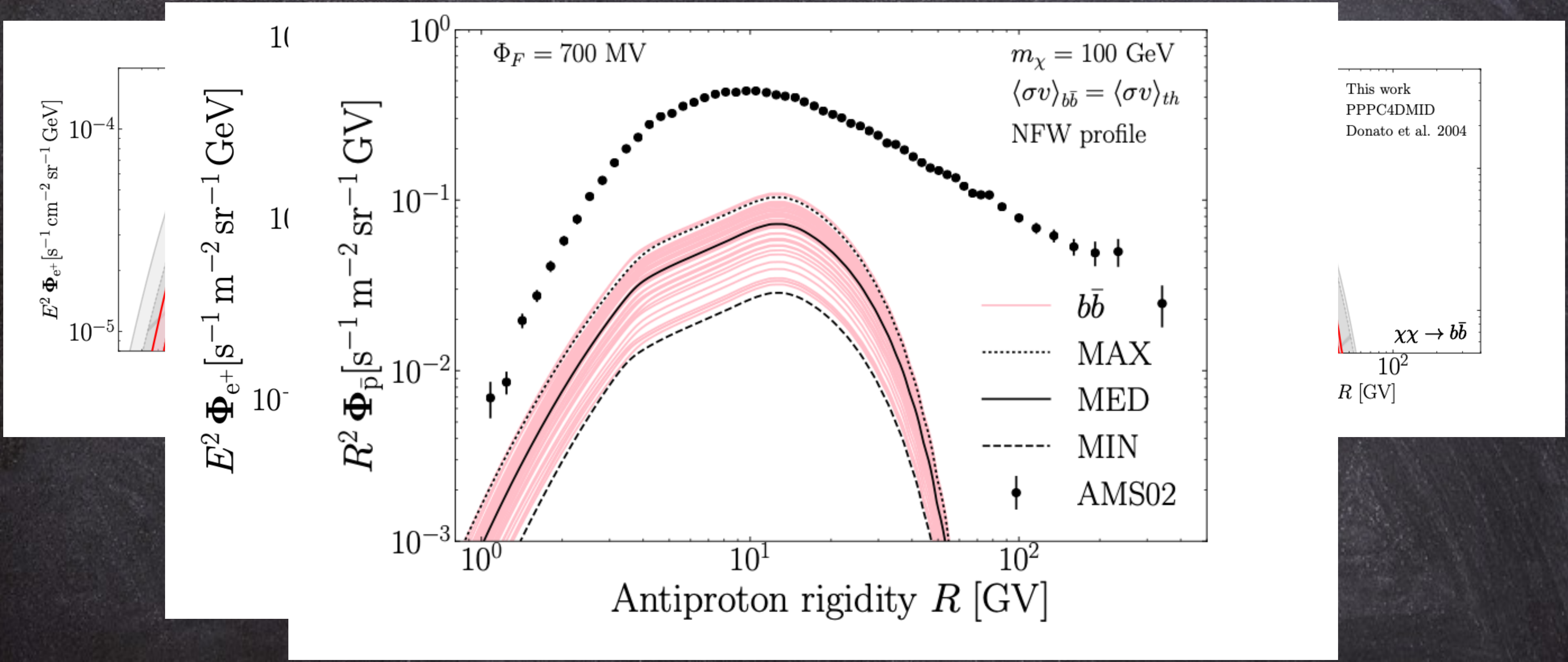

Uncertainty due to propagation now reduced to ~ 5
For GAPS physics a dedicated low energy study is mandatory (FD+, in progress)

Comparison with Monte Carlo generators

Koldobskiy et al., 2110.00496

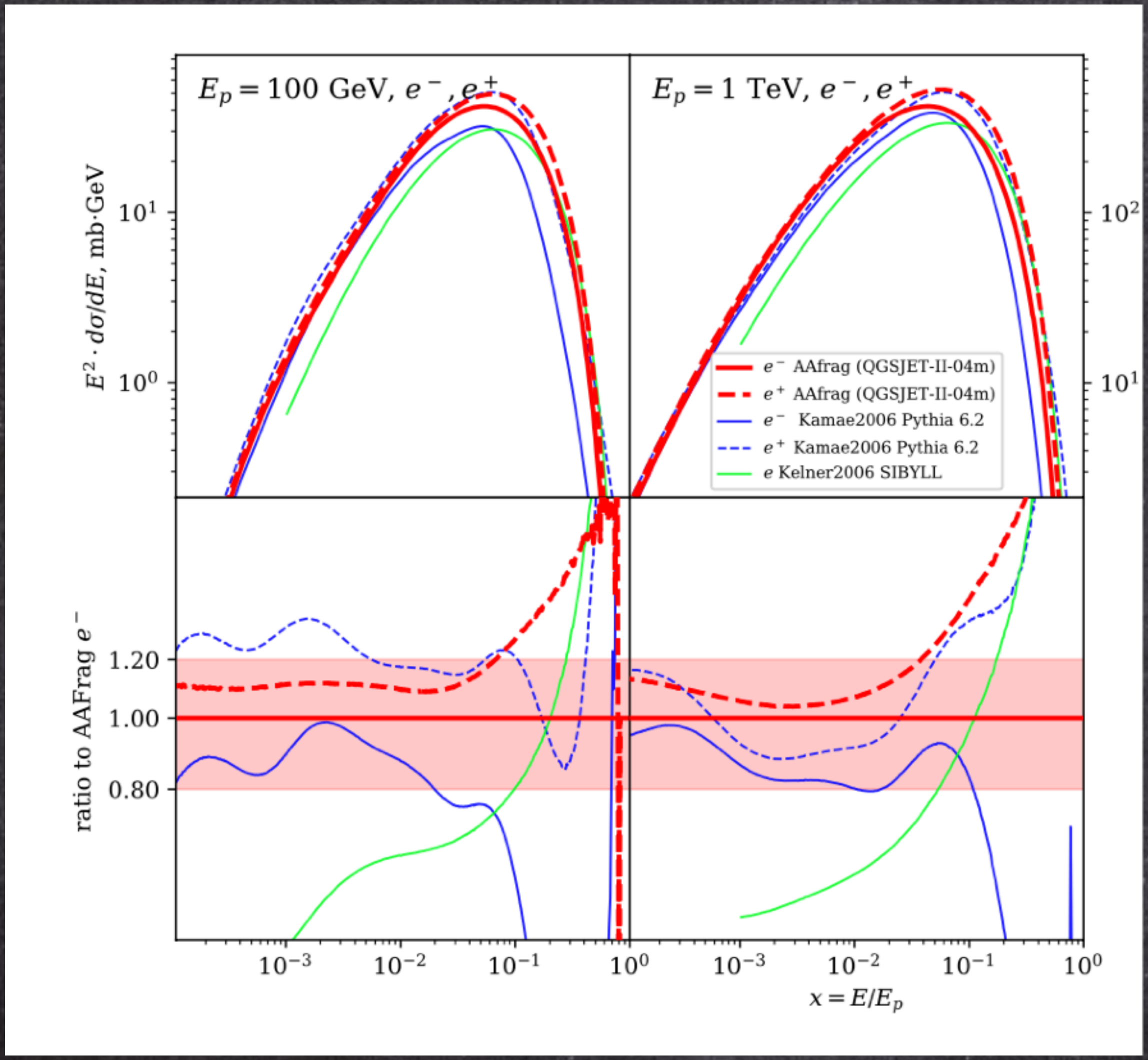

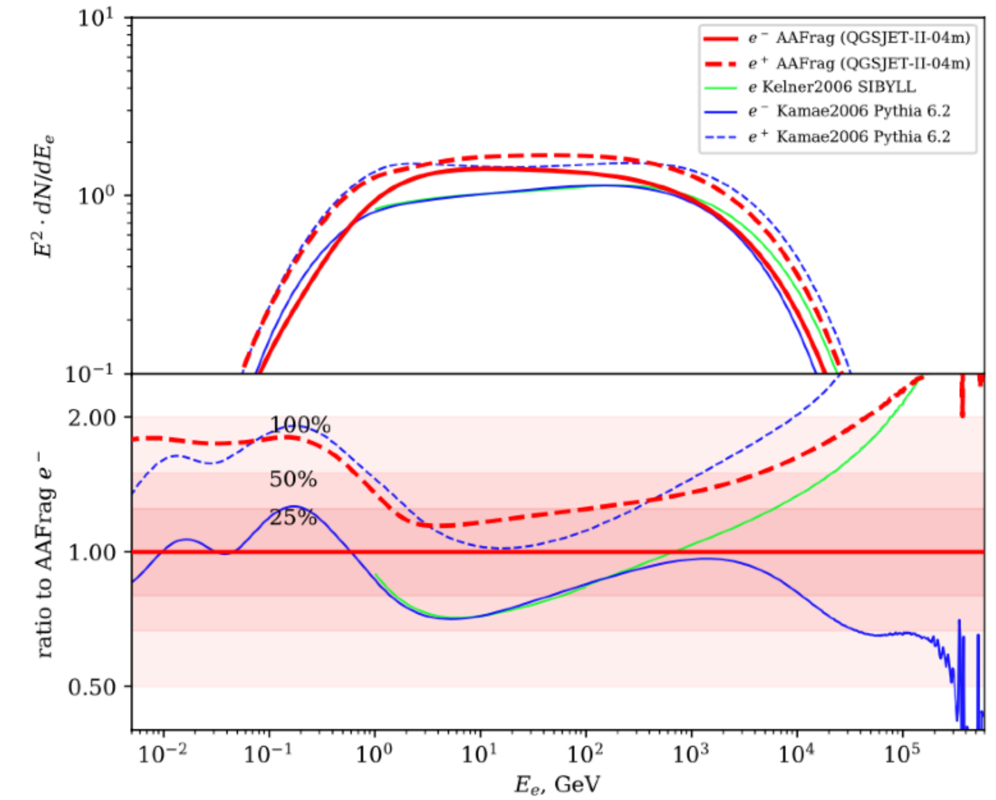

FIG. 9: Electron and positron fluxes for a power-law cosmic ray spectrum ($\propto 1/p^2 \exp(-p/p_0)$) .

Different MC modelings lead to considerable differences in the Production cross section, and consequently on the source spectrum

Fluka MC generator

N. Mazziotta+, AP 2017

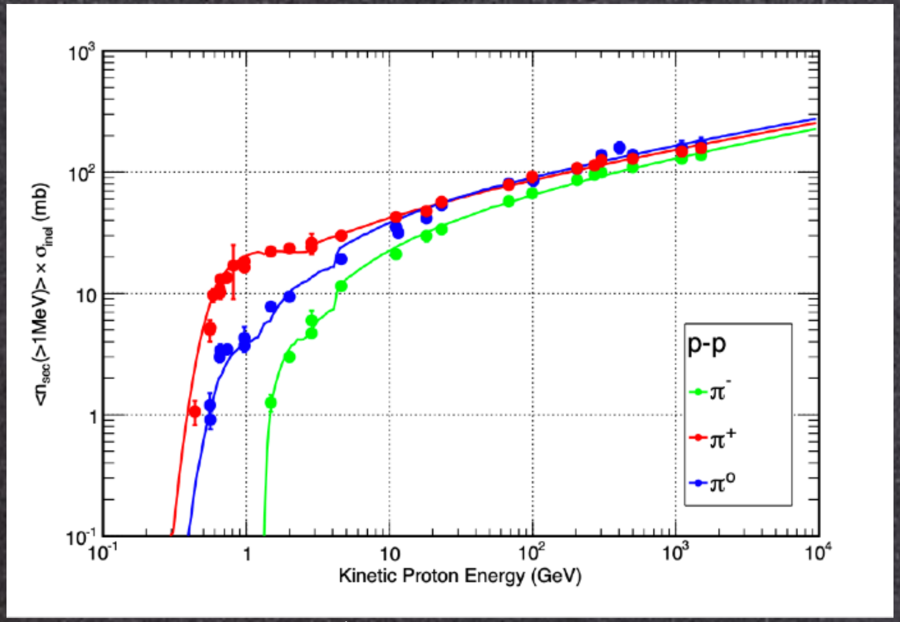

Points are from Dermer 1986

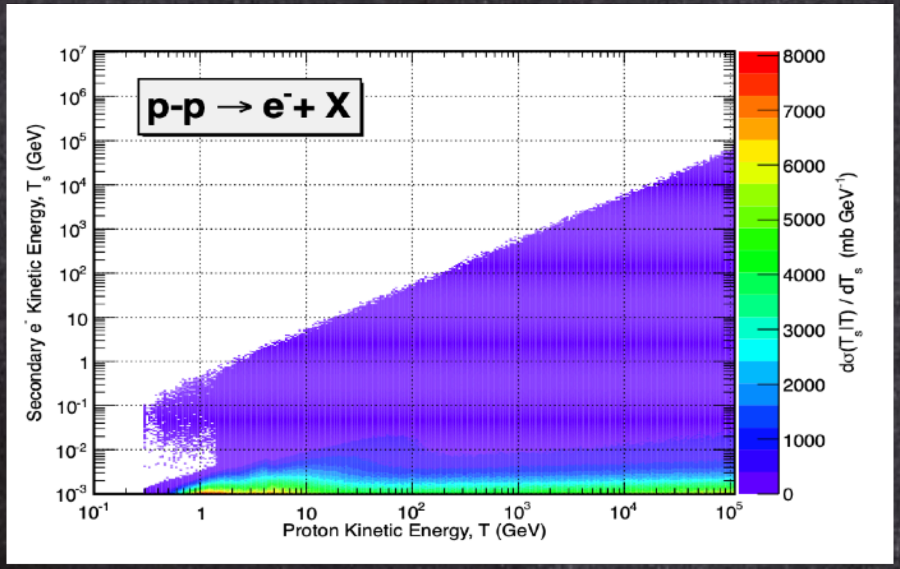

T_e is severely degraded from Projectile energy

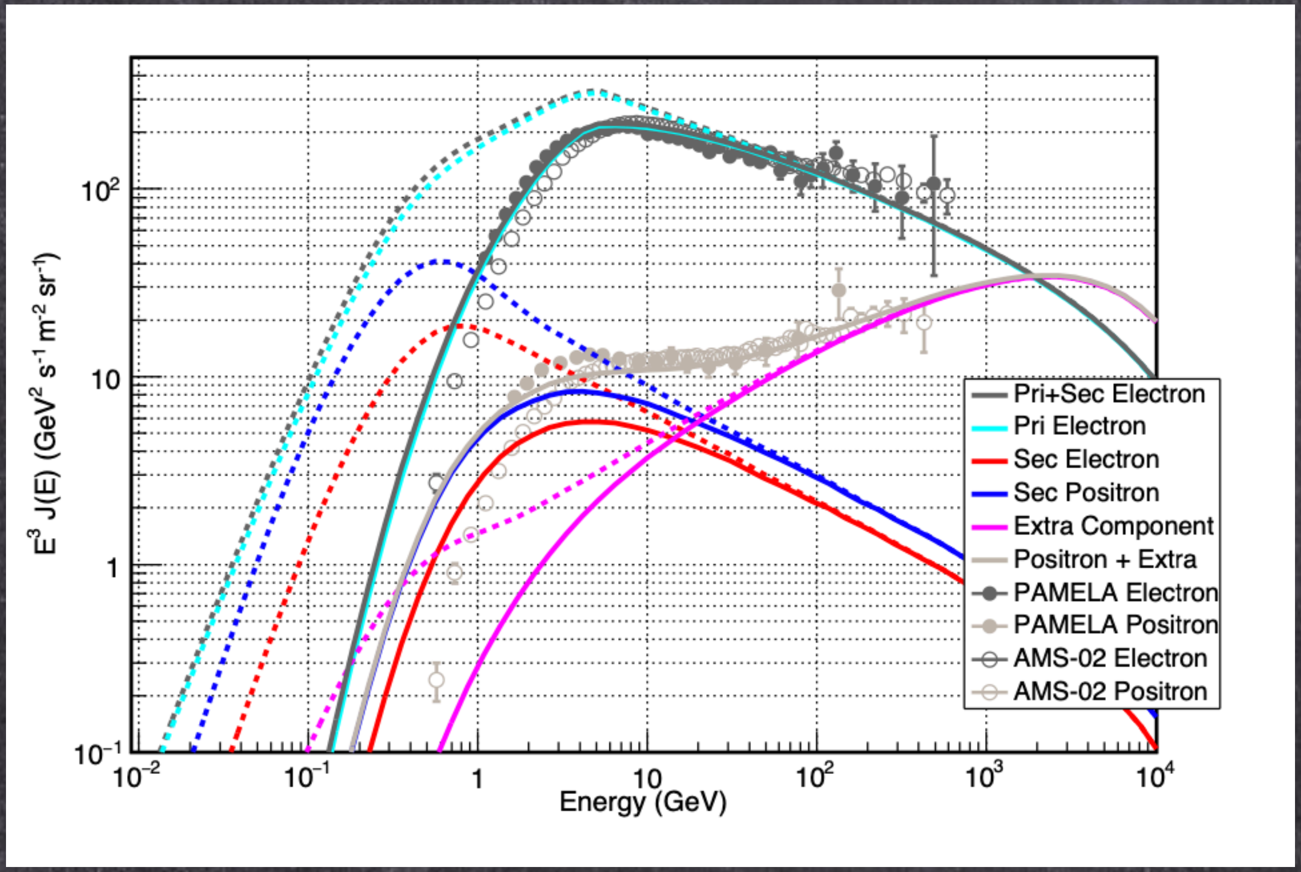

Propagated e+ and e- w.r.t. data

The case for Antideuterons

Antideuteron production in p-p collisions

Serksnyte et al,PRD 2022

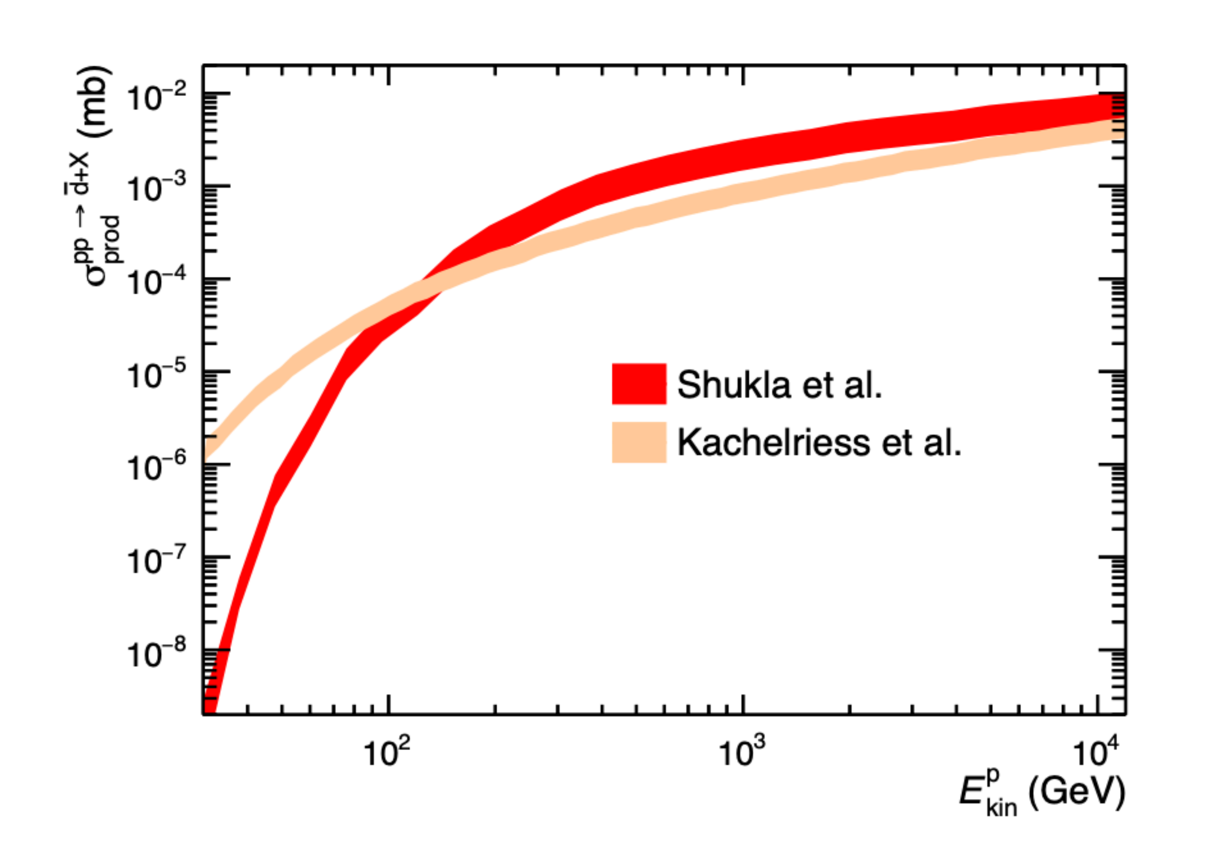

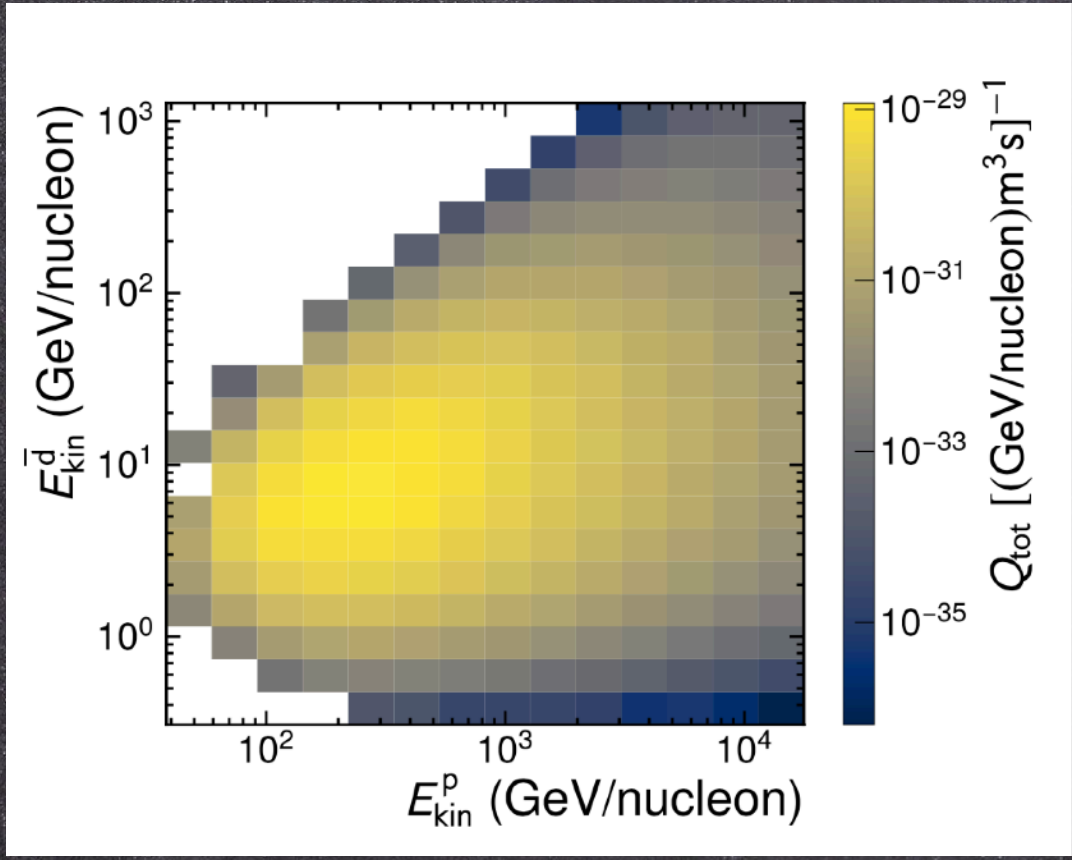

(L) Event-by-event (Monte Carlo) generators and coalescence models different generators may lead to significantly different predictions for low energy antideuterons.

(R) Secondary antideuterons below 1GeV/n are strongly suppressed

Antideuterons persepctives

P. Von Doetinchem et al. Phys. Rep. 2021

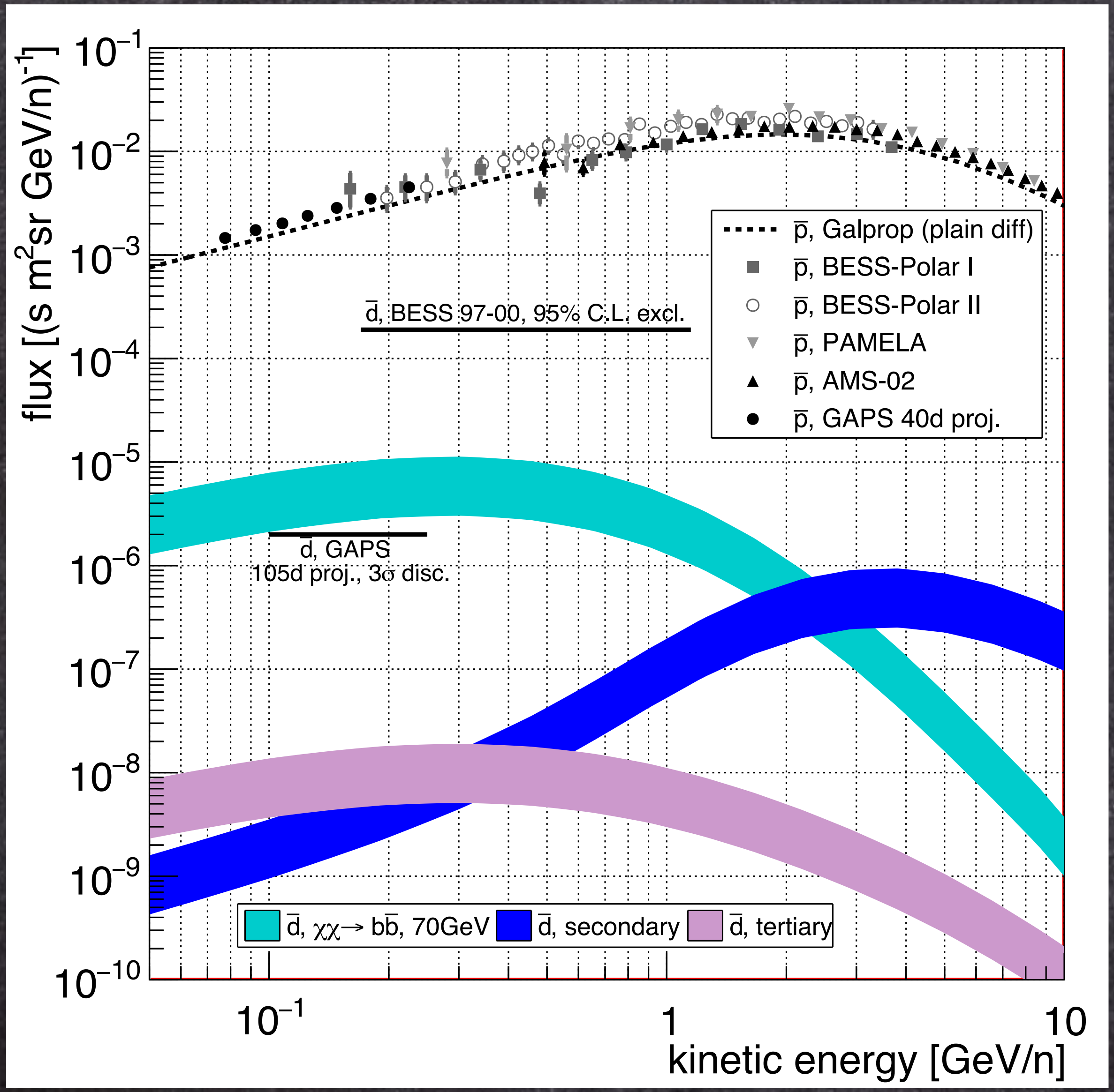

AMS-02 antiproton data

Antideuteron predictions for DM model indicated by pbar AMS-02 data

Bands are for coalescence uncertainty

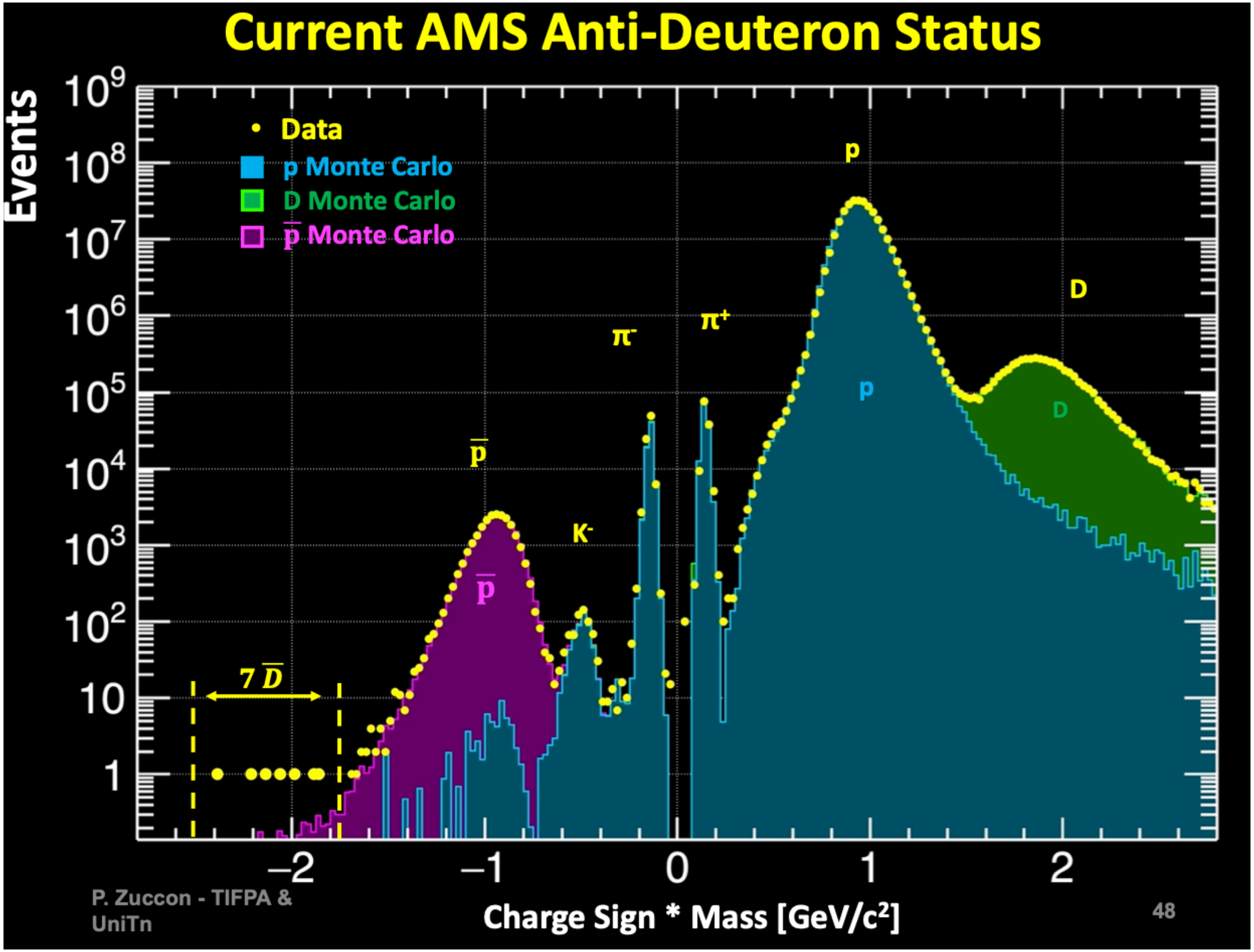

Current AMS Anti-Deuteron Status
Events
Data
p Monte Carlo
D Monte Carlo
p̄ Monte Carlo
p
D
π-
π+
p̄
K-
7 D̄
Charge Sign * Mass [GeV/c²]
P. Zuccon - TIFPA & UniTn
48

Models for p-n fusion into D

Statistical models, but they do not provide any dynamical clue

COALESCENCE models predict momentum distributions

- Uncorrelated $E_{\bar{d}} \frac{d^3 N_{\bar{d}}}{dp^3_{\bar{d}}} \simeq B_2 \left(E_{\bar{p}} \frac{d^3 N_{\bar{p}}}{dp^3_{\bar{p}}} \right) \left(E_{\bar{n}} \frac{d^3 N_{\bar{n}}}{dp^3_{\bar{n}}} \right)$

Simplest requirement: $|\vec{p}_{\bar{p}} - \vec{p}_{\bar{n}}| < p_0$ --> factorized coalescence (B_2 or P_C)

- Correlated, Monte Carlo based models. Particles close in momentum and physical space.

- Wigner function representations - semi-classical, wave functions

Coalescence according to Wigner functions

Kachelrieß, Ostapchenko, Tjemsland JCAP 2019; EJPA 2020

Given an antideuteron wave function, the fusion yield depends on one single parameter sizing the spatial spread of the two antinucleons

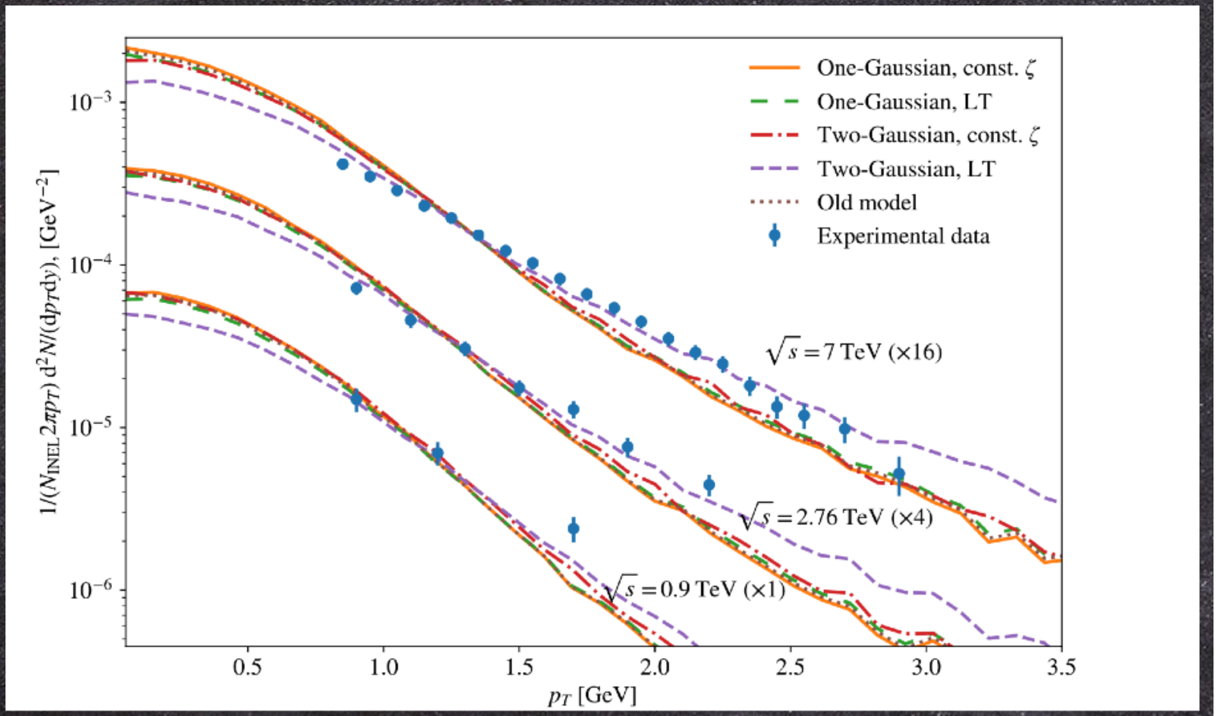

Fit to Alice data is good

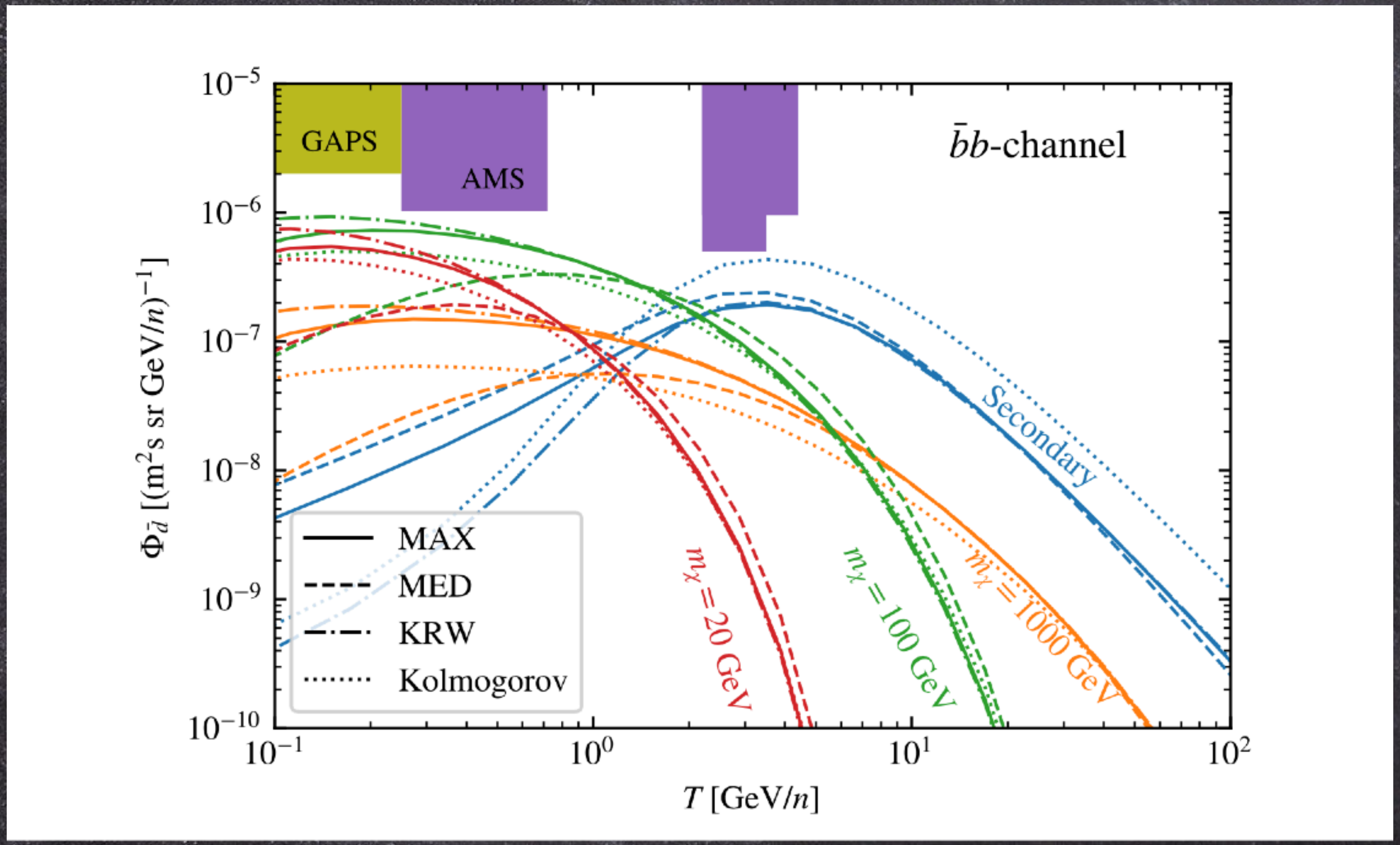

<σv> bound by antiprotons

Possible antideuteron verification of Dark Matter hint in antiprotons

FD, Fornengo, Korsmeier, PRD 2018

P_{coal} = 124 (62) MeV

P_{coal} = 248 (124) MeV

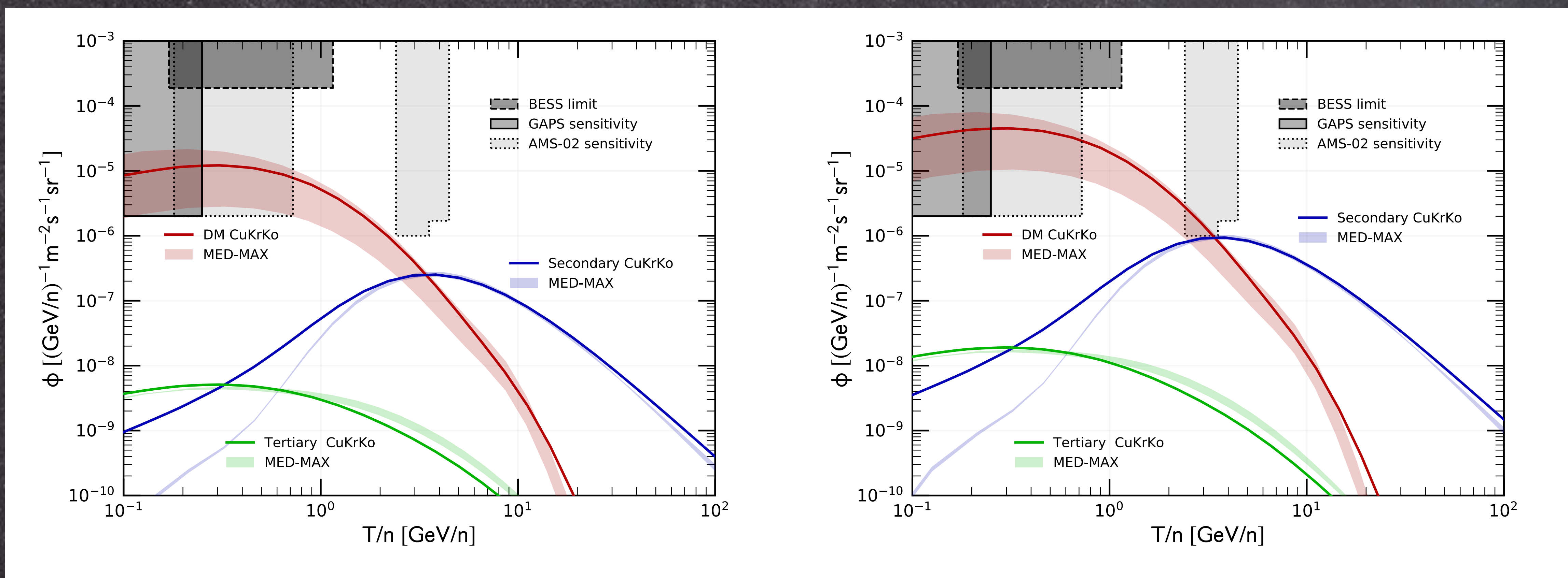

DM antiprotons possibly hidden in AMS data are potentially testable by AMS and GAPS

Current status and desired accuracy of the isotopic production cross sections relevant to astrophysics of cosmic rays I. Li, Be, B, C, N

Yoann Génolini*
Service de Physique Théorique, Université Libre de Bruxelles, Boulevard du Triomphe, CP225, 1050 Brussels, Belgium

David Maurin†
LPSC, Université Grenoble-Alpes, CNRS/IN2P3, 53 avenue des Martyrs, 38026 Grenoble, France

Igor V. Moskalenko‡
W. W. Hansen Experimental Physics Laboratory and Kavli Institute for Particle Astrophysics and Cosmology, Stanford University, Stanford, CA 94305, USA

Michael Unger§
Karlsruhe Institute of Technology, Karlsruhe, Germany

(Dated: March 14, 2018)

- Ranking of the most important cross sections for the production of Li, Be, B, C, N

- Propagation of uncertainties

Reaction $a+b\to c$	Flux impact f_{abc} [%] min	mean	max	σ [mb] range	Data	σ^c/σ
$\sigma(^{12}\mathrm{C}+\mathrm{H}\to{}^{6}\mathrm{Li})$	11.0	**13.6**	16.0	14.0	✓	
$\sigma(^{16}\mathrm{O}+\mathrm{H}\to{}^{6}\mathrm{Li})$	11.0	**13.5**	16.0	13.0	✓	
$\sigma(^{12}\mathrm{C}+\mathrm{H}\to{}^{7}\mathrm{Li})$	10.0	**11.9**	14.0	12.6	✓	
$\sigma(^{16}\mathrm{O}+\mathrm{H}\to{}^{7}\mathrm{Li})$	9.6	**11.3**	13.0	11.2	✓	
$\sigma(^{11}\mathrm{B}+\mathrm{H}\to{}^{7}\mathrm{Li})$	3.00	**3.52**	4.00	21.5	✓	
$\sigma(^{13}\mathrm{C}+\mathrm{H}\to{}^{7}\mathrm{Li})$	2.00	**2.39**	2.80	22.1		
$\sigma(^{16}\mathrm{O}+\mathrm{He}\to{}^{6}\mathrm{Li})$	2.00	**2.38**	2.80	20.6		
$\sigma(^{7}\mathrm{Li}+\mathrm{H}\to{}^{6}\mathrm{Li})$	2.30	**2.35**	2.40	31.5	✓	
$\sigma(^{12}\mathrm{C}+\mathrm{He}\to{}^{6}\mathrm{Li})$	1.90	**2.33**	2.70	21.6		
$\sigma(^{15}\mathrm{N}+\mathrm{H}\to{}^{7}\mathrm{Li})$	1.90	**2.27**	2.60	18.6	✓	
$\sigma(^{12}\mathrm{C}+\mathrm{He}\to{}^{7}\mathrm{Li})$	1.70	**2.04**	2.40	19.4		
$\sigma(^{16}\mathrm{O}+\mathrm{He}\to{}^{7}\mathrm{Li})$	1.70	**2.00**	2.30	17.8		
$\sigma(^{24}\mathrm{Mg}+\mathrm{H}\to{}^{6}\mathrm{Li})$	1.70	**1.98**	2.30	12.6		
$\sigma(^{13}\mathrm{C}+\mathrm{H}\to{}^{6}\mathrm{Li})$	1.60	**1.97**	2.30	17.8		
$\sigma(^{24}\mathrm{Mg}+\mathrm{H}\to{}^{7}\mathrm{Li})$	1.50	**1.74**	2.00	11.4		
$\sigma(^{10}\mathrm{B}+\mathrm{H}\to{}^{6}\mathrm{Li})$	1.40	**1.64**	1.90	20.0		
$\sigma(^{14}\mathrm{N}+\mathrm{H}\to{}^{6}\mathrm{Li})$	1.40	**1.62**	1.90	13.0	✓	
$\sigma(^{15}\mathrm{N}+\mathrm{H}\to{}^{6}\mathrm{Li})$	1.30	**1.60**	1.90	12.8	✓	
$\sigma(^{12}\mathrm{C}+\mathrm{H}\to{}^{11}\mathrm{B})$	1.20	**1.38**	1.60	30.0	✓	1.8
$\sigma(^{7}\mathrm{Be}+\mathrm{H}\to{}^{6}\mathrm{Li})$	1.20	**1.34**	1.50	21.0		
$\sigma(\mathbf{^{12}C+H\to{}^{11}C})$	1.10	**1.24**	1.40	26.9	✓	**n/a**
$\sigma(^{14}\mathrm{N}+\mathrm{H}\to{}^{7}\mathrm{Li})$	0.95	**1.13**	1.30	9.3	✓	
$\sigma(^{56}\mathrm{Fe}+\mathrm{H}\to{}^{7}\mathrm{Li})$	0.00	**0.94**	1.90	[0.0, 23.0]		
$\sigma(^{56}\mathrm{Fe}+\mathrm{H}\to{}^{6}\mathrm{Li})$	0.00	**0.94**	1.90	[0.0, 22.0]		
$\sigma(^{16}\mathrm{O}+\mathrm{H}\to{}^{11}\mathrm{B})$	0.80	**0.90**	1.00	18.2	✓	1.5
$\sigma(^{11}\mathrm{B}+\mathrm{H}\to{}^{6}\mathrm{Li})$	0.71	**0.84**	0.97	5.0	✓	
$\sigma(^{28}\mathrm{Si}+\mathrm{H}\to{}^{6}\mathrm{Li})$	0.00	**0.80**	1.60	[0.0, 13.0]		
$\sigma(^{10}\mathrm{B}+\mathrm{H}\to{}^{7}\mathrm{Li})$	0.70	**0.80**	0.90	10.0		
$\sigma(^{28}\mathrm{Si}+\mathrm{H}\to{}^{7}\mathrm{Li})$	0.00	**0.71**	1.40	[0.0, 11.0]		
$\sigma(^{16}\mathrm{O}+\mathrm{H}\to{}^{15}\mathrm{N})$	0.57	**0.64**	0.71	34.3	✓	1.8
$\sigma(^{12}\mathrm{C}+\mathrm{H}\to{}^{10}\mathrm{B})$	0.53	**0.64**	0.74	12.3	✓	1.1
$\sigma(^{20}\mathrm{Ne}+\mathrm{H}\to{}^{6}\mathrm{Li})$	0.00	**0.63**	1.30	[0.0, 13.0]		
$\sigma(\mathbf{^{16}O+H\to{}^{13}O})$	0.55	**0.63**	0.71	30.5	✓	**n/a**
$\sigma(^{16}\mathrm{O}+\mathrm{H}\to{}^{10}\mathrm{B})$	0.50	**0.60**	0.70	10.9	✓	
$\sigma(^{11}\mathrm{B}+\mathrm{He}\to{}^{7}\mathrm{Li})$	0.52	**0.60**	0.69	33.2		
$\sigma(\mathbf{^{16}O+H\to{}^{15}O})$	0.51	**0.57**	0.63	30.5	✓	**n/a**
$\sigma(^{20}\mathrm{Ne}+\mathrm{H}\to{}^{7}\mathrm{Li})$	0.00	**0.56**	1.10	[0.0, 11.0]		
$\sigma(^{16}\mathrm{O}+\mathrm{H}\to{}^{7}\mathrm{Be})$	0.37	**0.45**	0.54	10.0	✓	
$\sigma(\mathbf{^{16}O+H\to{}^{11}C})$	0.40	**0.45**	0.50	9.1		**n/a**
$\sigma(^{56}\mathrm{Fe}+\mathrm{He}\to{}^{7}\mathrm{Li})$	0.00	**0.44**	0.88	[0.0, 97.0]		
$\sigma(^{56}\mathrm{Fe}+\mathrm{He}\to{}^{6}\mathrm{Li})$	0.00	**0.44**	0.88	[0.0, 95.0]		
$\sigma(^{7}\mathrm{Li}+\mathrm{He}\to{}^{6}\mathrm{Li})$	0.42	**0.43**	0.45	52.2		
$\sigma(^{13}\mathrm{C}+\mathrm{He}\to{}^{7}\mathrm{Li})$	0.34	**0.41**	0.48	34.2		
$\sigma(^{12}\mathrm{C}+\mathrm{H}\to{}^{7}\mathrm{Be})$	0.34	**0.41**	0.48	9.7	✓	
$\sigma(^{16}\mathrm{O}+\mathrm{H}\to{}^{13}\mathrm{C})$	0.36	**0.41**	0.46	17.5	✓	1.2
$\sigma(^{24}\mathrm{Mg}+\mathrm{He}\to{}^{6}\mathrm{Li})$	0.33	**0.39**	0.46	22.5		
$\sigma(^{15}\mathrm{N}+\mathrm{He}\to{}^{7}\mathrm{Li})$	0.33	**0.39**	0.45	28.6		
$\sigma(\mathbf{^{7}Li+H\to{}^{6}He})$	0.00	**0.38**	0.76	[0.0, 10.0]		**n/a**
$\sigma(^{11}\mathrm{B}+\mathrm{H}\to{}^{10}\mathrm{B})$	0.29	**0.35**	0.40	38.9	✓	
$\sigma(^{24}\mathrm{Mg}+\mathrm{He}\to{}^{7}\mathrm{Li})$	0.29	**0.34**	0.40	20.3		
$\sigma(^{13}\mathrm{C}+\mathrm{He}\to{}^{6}\mathrm{Li})$	0.28	**0.34**	0.40	27.5		
$\sigma(\mathbf{^{56}Fe+H\to{}^{6}He})$	0.00	**0.29**	0.57	[0.0, 6.9]		**n/a**

Reaction $a+b\to c$	Flux impact f_{abc} [%] min	mean	max	σ [mb] range	Data	σ^c/σ
$\sigma(^{16}\mathrm{O}+\mathrm{H}\to{}^{7}\mathrm{Be})$	17.0	**17.6**	19.0	10.0	✓	
$\sigma(^{12}\mathrm{C}+\mathrm{H}\to{}^{7}\mathrm{Be})$	15.0	**15.9**	17.0	9.7	✓	
$\sigma(^{12}\mathrm{C}+\mathrm{H}\to{}^{9}\mathrm{Be})$	8.80	**9.27**	9.80	6.8	✓	
$\sigma(^{16}\mathrm{O}+\mathrm{H}\to{}^{9}\mathrm{Be})$	5.00	**5.34**	5.60	3.7	✓	
$\sigma(^{16}\mathrm{O}+\mathrm{He}\to{}^{7}\mathrm{Be})$	2.70	**2.87**	3.00	14.7		
$\sigma(^{28}\mathrm{Si}+\mathrm{H}\to{}^{7}\mathrm{Be})$	2.60	**2.77**	2.90	10.8		
$\sigma(^{24}\mathrm{Mg}+\mathrm{H}\to{}^{7}\mathrm{Be})$	2.50	**2.65**	2.80	10.0		
$\sigma(^{12}\mathrm{C}+\mathrm{He}\to{}^{7}\mathrm{Be})$	2.30	**2.48**	2.60	13.7		
$\sigma(^{11}\mathrm{B}+\mathrm{H}\to{}^{9}\mathrm{Be})$	2.30	**2.36**	2.50	10.0	✓	
$\sigma(^{12}\mathrm{C}+\mathrm{H}\to{}^{10}\mathrm{Be})$	2.00	**2.16**	2.30	4.0	✓	
$\sigma(^{14}\mathrm{N}+\mathrm{H}\to{}^{7}\mathrm{Be})$	2.00	**2.12**	2.20	10.1	✓	
$\sigma(^{20}\mathrm{Ne}+\mathrm{H}\to{}^{7}\mathrm{Be})$	1.60	**1.73**	1.90	[7.4, 9.7]		
$\sigma(^{10}\mathrm{B}+\mathrm{H}\to{}^{9}\mathrm{Be})$	1.60	**1.62**	1.70	13.9		
$\sigma(^{12}\mathrm{C}+\mathrm{He}\to{}^{9}\mathrm{Be})$	1.40	**1.45**	1.50	9.6		
$\sigma(^{12}\mathrm{C}+\mathrm{H}\to{}^{11}\mathrm{B})$	1.30	**1.43**	1.60	30.0	✓	1.8
$\sigma(^{15}\mathrm{N}+\mathrm{H}\to{}^{9}\mathrm{Be})$	1.20	**1.29**	1.40	7.3	✓	
$\sigma(\mathbf{^{12}C+H\to{}^{11}C})$	1.20	**1.28**	1.40	26.9	✓	**n/a**
$\sigma(^{16}\mathrm{O}+\mathrm{H}\to{}^{10}\mathrm{Be})$	1.20	**1.27**	1.40	2.2	✓	
$\sigma(^{11}\mathrm{B}+\mathrm{H}\to{}^{10}\mathrm{Be})$	1.10	**1.21**	1.30	12.9	✓	
$\sigma(^{11}\mathrm{B}+\mathrm{H}\to{}^{7}\mathrm{Be})$	0.99	**1.16**	1.30	[3.6, 4.5]	✓	
$\sigma(^{15}\mathrm{N}+\mathrm{H}\to{}^{7}\mathrm{Be})$	1.10	**1.15**	1.20	5.4	✓	
$\sigma(^{13}\mathrm{C}+\mathrm{H}\to{}^{9}\mathrm{Be})$	0.96	**1.03**	1.10	6.7	✓	
$\sigma(^{28}\mathrm{Si}+\mathrm{H}\to{}^{9}\mathrm{Be})$	0.91	**0.96**	1.00	4.5	✓	
$\sigma(^{10}\mathrm{B}+\mathrm{H}\to{}^{7}\mathrm{Be})$	0.93	**0.95**	0.98	6.9	✓	
$\sigma(^{24}\mathrm{Mg}+\mathrm{H}\to{}^{9}\mathrm{Be})$	0.89	**0.94**	0.99	4.3		
$\sigma(^{16}\mathrm{O}+\mathrm{H}\to{}^{11}\mathrm{B})$	0.87	**0.94**	1.00	18.2	✓	1.5
$\sigma(^{56}\mathrm{Fe}+\mathrm{H}\to{}^{7}\mathrm{Be})$	0.11	**0.92**	1.70	[0.6, 11.0]		
$\sigma(^{16}\mathrm{O}+\mathrm{He}\to{}^{9}\mathrm{Be})$	0.82	**0.87**	0.92	5.4		
$\sigma(^{13}\mathrm{C}+\mathrm{H}\to{}^{7}\mathrm{Be})$	0.71	**0.76**	0.81	4.1	✓	
$\sigma(^{20}\mathrm{Ne}+\mathrm{H}\to{}^{9}\mathrm{Be})$	0.68	**0.72**	0.76	4.3		
$\sigma(^{12}\mathrm{C}+\mathrm{H}\to{}^{10}\mathrm{B})$	0.59	**0.64**	0.68	12.3	✓	1.1
$\sigma(^{16}\mathrm{O}+\mathrm{H}\to{}^{10}\mathrm{B})$	0.56	**0.60**	0.65	10.9	✓	
$\sigma(^{9}\mathrm{Be}+\mathrm{H}\to{}^{7}\mathrm{Be})$	0.59	**0.59**	0.60	10.6	✓	
$\sigma(^{28}\mathrm{Si}+\mathrm{He}\to{}^{7}\mathrm{Be})$	0.53	**0.56**	0.60	19.8		
$\sigma(^{56}\mathrm{Fe}+\mathrm{H}\to{}^{9}\mathrm{Be})$	0.06	**0.53**	1.00	[0.4, 7.5]		
$\sigma(^{24}\mathrm{Mg}+\mathrm{He}\to{}^{7}\mathrm{Be})$	0.47	**0.50**	0.52	16.8		
$\sigma(\mathbf{^{16}O+H\to{}^{11}C})$	0.43	**0.47**	0.50	9.1		**n/a**
$\sigma(^{16}\mathrm{O}+\mathrm{H}\to{}^{15}\mathrm{N})$	0.41	**0.44**	0.47	34.3	✓	1.8
$\sigma(^{56}\mathrm{Fe}+\mathrm{He}\to{}^{7}\mathrm{Be})$	0.05	**0.41**	0.77	[2.4, 43.0]		
$\sigma(\mathbf{^{16}O+H\to{}^{15}O})$	0.37	**0.39**	0.42	30.5	✓	**n/a**
$\sigma(^{27}\mathrm{Al}+\mathrm{H}\to{}^{7}\mathrm{Be})$	0.30	**0.38**	0.45	[5.3, 8.9]		
$\sigma(^{14}\mathrm{N}+\mathrm{H}\to{}^{9}\mathrm{Be})$	0.35	**0.37**	0.39	2.1	✓	
$\sigma(^{11}\mathrm{B}+\mathrm{He}\to{}^{9}\mathrm{Be})$	0.35	**0.37**	0.38	14.0		
$\sigma(^{13}\mathrm{C}+\mathrm{H}\to{}^{10}\mathrm{Be})$	0.33	**0.37**	0.40	5.9	✓	
$\sigma(^{23}\mathrm{Na}+\mathrm{H}\to{}^{7}\mathrm{Be})$	0.30	**0.35**	0.41	[5.8, 8.6]		
$\sigma(^{11}\mathrm{B}+\mathrm{H}\to{}^{10}\mathrm{B})$	0.33	**0.35**	0.37	38.9	✓	
$\sigma(^{25}\mathrm{Mg}+\mathrm{H}\to{}^{7}\mathrm{Be})$	0.29	**0.34**	0.40	[5.6, 8.8]		
$\sigma(^{12}\mathrm{C}+\mathrm{He}\to{}^{10}\mathrm{Be})$	0.31	**0.34**	0.36	5.6		
$\sigma(^{14}\mathrm{N}+\mathrm{He}\to{}^{7}\mathrm{Be})$	0.32	**0.34**	0.36	14.4		
$\sigma(^{20}\mathrm{Ne}+\mathrm{He}\to{}^{7}\mathrm{Be})$	0.28	**0.30**	0.32	[12.0, 15.0]		
$\sigma(^{22}\mathrm{Ne}+\mathrm{H}\to{}^{7}\mathrm{Be})$	0.22	**0.25**	0.28	[4.7, 6.4]		
$\sigma(^{10}\mathrm{B}+\mathrm{He}\to{}^{9}\mathrm{Be})$	0.25	**0.25**	0.26	19.6		
$\sigma(^{26}\mathrm{Mg}+\mathrm{H}\to{}^{7}\mathrm{Be})$	0.21	**0.25**	0.29	[4.7, 7.2]		
$\sigma(\mathbf{^{16}O+H\to{}^{9}Li})$	0.23	**0.24**	0.26	0.3	✓	**n/a**

# of channels	in range	contribution [%]
13	[1%,100%]	82.2
25	[0.1%,1%]	7.7
110	[0.01%,0.1%]	3.8
346	[0.001%,0.01%]	1.3
526	[0.0001%,0.001%]	0.2
2340	[0.0%,0.0001%]	0.0

Channel	min	mean	max
$^{12}\mathrm{C}\to{}^{11}\mathrm{B}$	30.8	**32.7**	35.3
$^{16}\mathrm{O}\to{}^{11}\mathrm{B}$	16.2	**17.7**	18.8
$^{12}\mathrm{C}\to{}^{10}\mathrm{B}$	9.04	**9.95**	10.9
$^{16}\mathrm{O}\to{}^{10}\mathrm{B}$	7.64	**8.17**	8.68
$^{12}\mathrm{C}\to{}^{11}\mathrm{B}\to{}^{10}\mathrm{B}$	2.07	**2.16**	2.26
$^{16}\mathrm{O}\to{}^{12}\mathrm{C}\to{}^{11}\mathrm{B}$	1.60	**1.96**	2.34
$^{16}\mathrm{O}\to{}^{15}\mathrm{N}\to{}^{11}\mathrm{B}$	1.29	**1.69**	2.04
$^{24}\mathrm{Mg}\to{}^{11}\mathrm{B}$	1.51	**1.59**	1.69
$^{20}\mathrm{Ne}\to{}^{11}\mathrm{B}$	1.26	**1.32**	1.39
$^{14}\mathrm{N}\to{}^{11}\mathrm{B}$	1.00	**1.32**	1.66
$^{28}\mathrm{Si}\to{}^{11}\mathrm{B}$	0.85	**1.29**	1.66
$^{16}\mathrm{O}\to{}^{11}\mathrm{B}\to{}^{10}\mathrm{B}$	1.03	**1.17**	1.26
$^{16}\mathrm{O}\to{}^{13}\mathrm{C}\to{}^{11}\mathrm{B}$	0.54	**1.15**	1.62
$^{16}\mathrm{O}\to{}^{14}\mathrm{N}\to{}^{11}\mathrm{B}$	0.68	**0.83**	0.92
$^{24}\mathrm{Mg}\to{}^{10}\mathrm{B}$	0.66	**0.75**	0.84
$^{16}\mathrm{O}\to{}^{12}\mathrm{C}\to{}^{10}\mathrm{B}$	0.51	**0.59**	0.69
$^{16}\mathrm{O}\to{}^{15}\mathrm{N}\to{}^{10}\mathrm{B}$	0.50	**0.59**	0.68
$^{20}\mathrm{Ne}\to{}^{10}\mathrm{B}$	0.47	**0.54**	0.63
$^{28}\mathrm{Si}\to{}^{10}\mathrm{B}$	0.32	**0.53**	0.67
$^{14}\mathrm{N}\to{}^{10}\mathrm{B}$	0.39	**0.50**	0.65
$^{56}\mathrm{Fe}\to{}^{11}\mathrm{B}$	0.11	**0.49**	1.10
$^{16}\mathrm{O}\to{}^{13}\mathrm{C}\to{}^{10}\mathrm{B}$	0.12	**0.32**	0.50
$^{16}\mathrm{O}\to{}^{14}\mathrm{N}\to{}^{10}\mathrm{B}$	0.26	**0.31**	0.36
$^{24}\mathrm{Mg}\to{}^{12}\mathrm{C}\to{}^{11}\mathrm{B}$	0.21	**0.22**	0.25
$^{56}\mathrm{Fe}\to{}^{10}\mathrm{B}$	0.00	**0.21**	0.71
$^{20}\mathrm{Ne}\to{}^{12}\mathrm{C}\to{}^{11}\mathrm{B}$	0.19	**0.20**	0.22
$^{14}\mathrm{N}\to{}^{12}\mathrm{C}\to{}^{11}\mathrm{B}$	0.14	**0.20**	0.25
$^{13}\mathrm{C}\to{}^{11}\mathrm{B}$	0.15	**0.18**	0.24
$^{28}\mathrm{Si}\to{}^{12}\mathrm{C}\to{}^{11}\mathrm{B}$	0.10	**0.18**	0.21
$^{25}\mathrm{Mg}\to{}^{11}\mathrm{B}$	0.14	**0.17**	0.19
$^{32}\mathrm{S}\to{}^{11}\mathrm{B}$	0.09	**0.14**	0.17
$^{26}\mathrm{Mg}\to{}^{11}\mathrm{B}$	0.11	**0.13**	0.14
$^{27}\mathrm{Al}\to{}^{11}\mathrm{B}$	0.08	**0.12**	0.16
$^{24}\mathrm{Mg}\to{}^{16}\mathrm{O}\to{}^{11}\mathrm{B}$	0.10	**0.12**	0.13
$^{24}\mathrm{Mg}\to{}^{23}\mathrm{Na}\to{}^{11}\mathrm{B}$	0.10	**0.11**	0.14
$^{20}\mathrm{Ne}\to{}^{15}\mathrm{N}\to{}^{11}\mathrm{B}$	0.09	**0.11**	0.12
$^{24}\mathrm{Mg}\to{}^{11}\mathrm{B}\to{}^{10}\mathrm{B}$	0.10	**0.11**	0.11
$^{20}\mathrm{Ne}\to{}^{16}\mathrm{O}\to{}^{11}\mathrm{B}$	0.09	**0.10**	0.12

Invaluable theoretical and experimental work to do for a correct understanding of precise CR data

Results on different sqrt(s)

L. Orusa, M. Di Mauro, FD, M. Korsmeier, PRD 2022

We use σ_{inv} or multiplicity

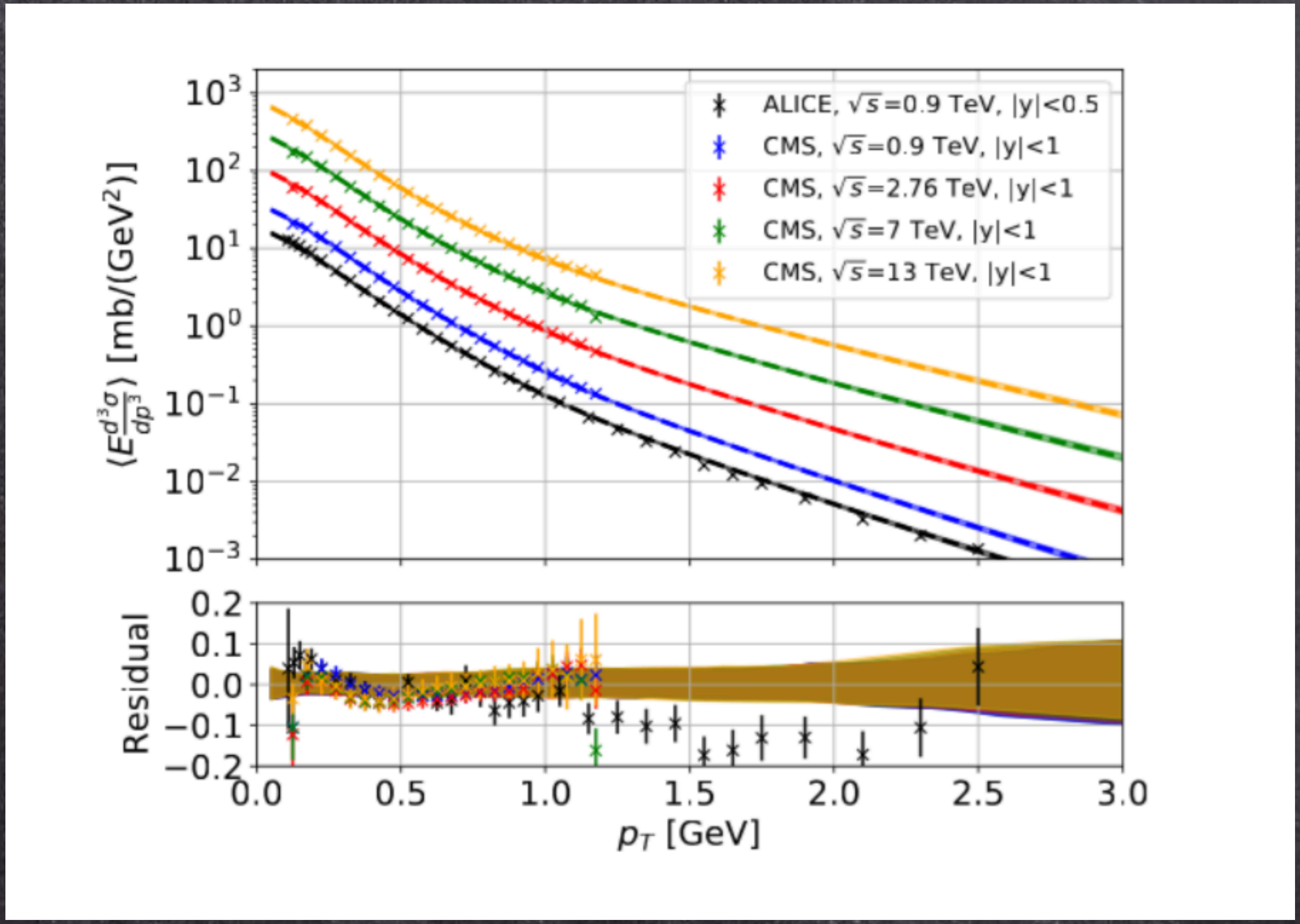

Uncertainties between 5 and 10% come from energy scaling